



INTERNATIONAL ATOMIC ENERGY AGENCY
UNITED NATIONS EDUCATIONAL, SCIENTIFIC AND CULTURAL ORGANIZATION



INTERNATIONAL CENTRE FOR THEORETICAL PHYSICS
34100 TRIESTE (ITALY) - P.O.B. 586 - MIRAMARE - STRADA COSTIERA 11 - TELEPHONE: 2240-1
CABLE: CENTRATOM - TELEX 460892-1

SMR.380/2

COLLEGE ON THEORETICAL AND EXPERIMENTAL RADIOPROPAGATION
SCIENCE

6 - 24 February 1989

Radio Noise Theory and Measurement

M. HAYAKAWA

Research Institute of Atmospherics, Nagoya University,
Toyokawa, Japan

These notes are intended for internal distribution only.

Contents

1. General description of radio noises
 - 1.1. Concept of radio noises
 - 1.2. Classification of radio noises
 - 1.3. Intensity of radio noises
 - 1.4. Frequency dependence of radio noises
2. Natural radio noise
 - 2.1. General description
 - 2.2. Atmospherics
 - 2.2.1. Different kinds of atmospherics
 - 2.2.2. Generation sources of atmospherics
 - 2.2.3. Diurnal and seasonal variations of atmospherics
 - 2.2.4. Frequency spectrum of atmospherics
 - 2.2.5. The waveforms of atmospherics
 - 2.2.6. Statistical properties of atmospherics
 - 2.3. Radio noises of extra-terrestrial origin
 - 2.3.1. General information
 - 2.3.2. Galactic and cosmic radio noise
 - 2.3.3. Discrete radio sources
 - 2.3.4. Radio noises from the solar system
3. Man-made noise
 - 3.1. General description
 - 3.2. Sources of man-made noises
 - 3.2.1. Unintentional man-made noise and intended coherent radiation
 - 3.2.2. Radio noises from power transmission and distribution line
 - 3.2.3. Automotive noise
 - 3.3. Composite city noise
4. Radio noises and the design of radio telecommunication system
 - 4.1. Threshold power at the receiver
 - 4.2. Predetection signal to noise ratio and operating noise figure
 - 4.3. Estimates of minimum(and maximum) environmental noise levels
 - 4.4. Example determination of required receiver noise figure
5. Internal noise
 - 5.1. Internal noise(receiver internal noise)
 - 5.2. Sensitivity of the receiver and the expression of internal noise
 - 5.3. Equivalent noise bandwidth of an amplifier
 - 5.4. Noise figure
 - 5.5. Signal to noise ratio and its improvement
6. Description of random noises and their measurements
 - 6.1. Measurement parameters
 - 6.2. Measurement techniques

1. General description of radio noise

1.1. Concept of radio noise

Fig.1.1-1 illustrates the significance and concept of radio noises on the telecommunication system, by indicating the situation where we convey the information(message or signal) to the receiver in the presence of radio noises. "Radio noises" are defined as the noises which are induced either during the telecommunication propagation path or at the receiving terminal of the electrical observing equipment, then making the message in an unpredictable condition. The end of the telecommunication link receives not only the wanted signal, but also unwanted signals which are not necessarily related with the wanted signals. These unwanted signals consist of the receiver's own internally generated noise, naturally occurring noises, man-made noises which reach the receiving antenna, and cross-talks from other telecommunication system. This composite interference environment, whether predominantly noise or unwanted signals, is referred to simply as "noises". The noise generated within the receiver is an example of the "internal noise", which is defined as being due to the electron phenomena. While, the natural noise with its origin either terrestrial or extra-terrestrial and man-made noises are called the "external noises" in contrast with the internal noise.

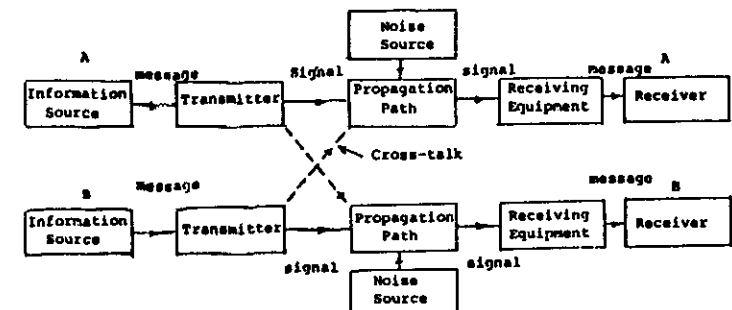


Fig.1.1-1 Concept of radio noises in the telecommunications

1.2. Classification of radio noises

Radio noises can be classified from the different points of view, but they are normally classified in the following way based either on the nature of the generation source or on the consideration of their waveforms.

(a) Classification in terms of generation sources:

Radio noise	natural noise	<ul style="list-style-type: none"> atmospheric radio noise cosmic noise(solar,planetary and galactic and extra-galactic radio stars) thermal noise
	man-made noise (different kinds of sparks,high frequency oscillation etc)	

(b) Classification in terms of waveforms (see Fig.1.2-1):

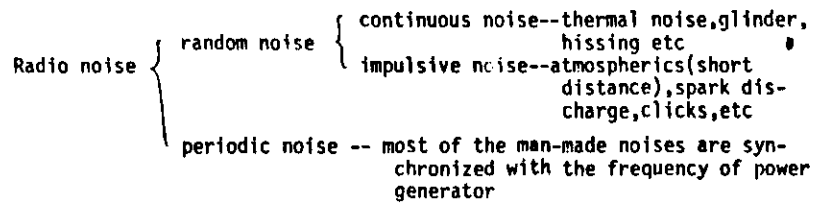
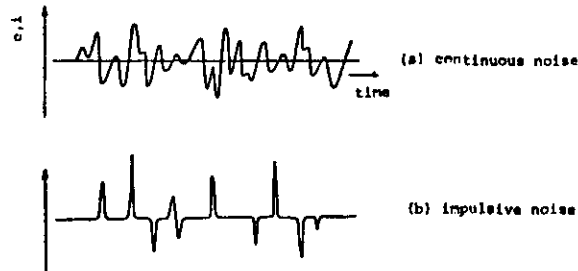


Fig.1.2-1 Classification of random noise based on waveforms



1.3. Intensity of radio noises

Radio noises are essentially random and complex in nature, and so it is necessary to make use of the statistical treatment when expressing quantitatively the characteristics of radio noises such as their intensity. In the following we give a brief description of the three basic quantities in order to indicate the intensity of radio noises.

(a) Electric field intensity:

Let the instantaneous value of electric field of radio noises for a particular polarization be expressed as $e_n(t)$, and then the effective value of the electric field is defined as $\langle e_n(t)^2 \rangle^{1/2}$ where the bracket indicates the time average. This effective value in this definition is dependent on the polarization, measuring system, bandwidth of the receiver, detection system, etc, and so it is necessary to specify these quantities as well. Other expressions for the electric field include, average value, quasi-peak value and so on.

(b) Poynting power (Power flux density):

Let us consider a cross section with unit area [m^2] perpendicular to the propagation direction of radio waves. Then, the power flux density W is defined as the energy flow of radio noises over a bandwidth of 1Hz, and W is related to the intensity of noise electric field e_n as follows.

$$W = (e_n)^2 / 120 \pi \quad [\text{W/m}^2] \quad (1.3-1)$$

If we receive the noises with a receiver having the bandwidth B and with the receiving antenna having the effective area A ,

the available power P_N is given by

$$P_N = A \cdot W \cdot B \quad [\text{W}] \quad (1.3-2)$$

(c) External noise figure, \overline{EN} :

Every electric conductor produces the noise voltage across its terminals as a result of the thermal motion of the free electrons in the conductor. This effect is referred to as thermal noise. The Nyquist theory indicates that the mean square value of the noise voltage is given by

$$\overline{e^2} = 4 \kappa T R B \quad (1.3-3)$$

where e is the thermal noise voltage[V] across the resistance $R[\Omega]$ at the absolute temperature $T[^\circ\text{K}]$, κ , Boltzmann constant, B , noise bandwidth[Hz]. So, this body is equivalently regarded as the noise generator with an internal resistance R , and then the available power of radio noise, P_N becomes,

$$P_N = \overline{e^2} / 4R \longrightarrow P_N = \kappa T B \quad [\text{W}] \quad (1.3-4)$$

This equation is Rayleigh-Jean's law and so the noise power can be expressed in terms of the equivalent noise temperature, $T[^\circ\text{K}]$. When W_a is the noise power received by a lossless, isotropic antenna and we put the corresponding noise temperature as T_a , the following relationship results in.

$$W_a = \kappa T_a B = F \kappa T_0 B \quad [\text{W}] \quad (1.3-5)$$

Then,

$$F = T_a / T_0 \quad [T_0 = 290^\circ\text{K}] \quad (1.3-6)$$

F is called the "effective external noise figure". In order to distinguish this external noise figure F from the internal noise figure to be discussed in 5.4, we usually describe this external noise figure as \overline{EN} .

1.4. Frequency dependence of radio noise

Radio noises are found to occupy a wide frequency range as shown in Fig.1.4-1. In the figure, we have plotted the frequency dependence of different kinds of radio noises including natural and man-made noises. The figure implies that we can expect that atmospherics play an important role in the frequency range below 10-20 MHz, while the dominant noise sources above VHF are extra-terrestrial radio noises and man-made urban noises. The noise level equal to κT_0 is also shown for the sake of comparison.

The detailed description of each radio noise will be given in the subsequent sections.

2 Natural Radio Noises

2.1. General description

The naturally occurring radio noise sources that dominate the radio-noise spectrum are summarized in Fig.2.1-1. The radiated power flux density is plotted in dB above $1 \text{ W/m}^2/\text{Hz}$ as a function of frequency for different kinds of natural noises. The important sources are generally found to be (1) atmospheric radio noises, (2) solar radio noises and (3) cosmic noise. The figure indicates that in the frequency range below 20 MHz, atmospheric noise (so-called "atmospherics") predominates over other natural sources in the temperate latitudes, and also that the most important noise source above VHF is cosmic noise. In the following we provide

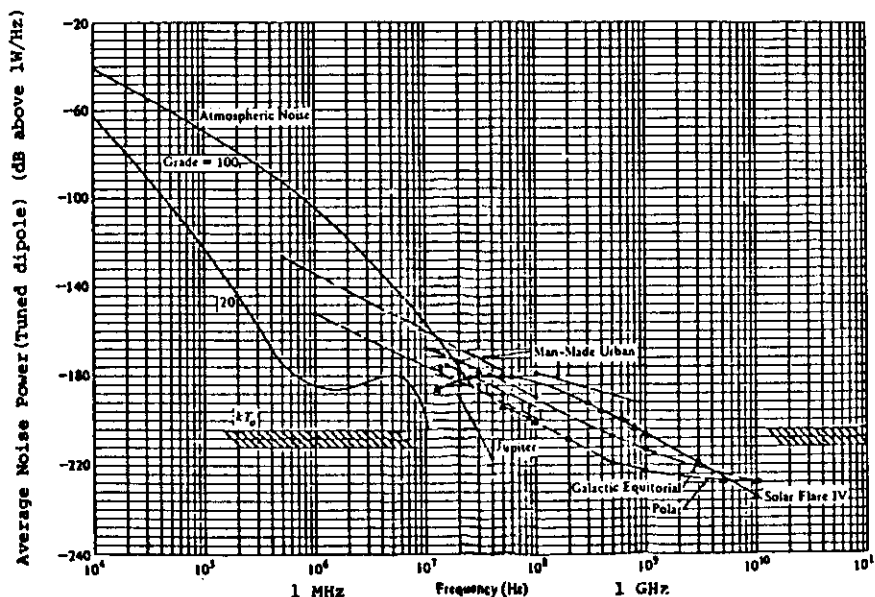


Fig.1.4-1 Average power of natural and man-made radio noise observed with a tuned dipole antenna

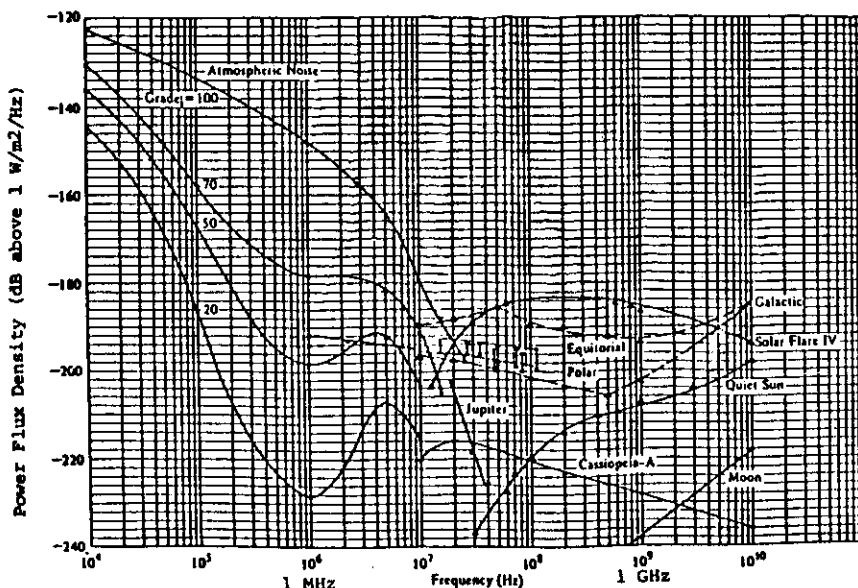


Fig.2.1-1 Power flux density of natural radio noise sources

you with more detailed description of the characteristics of each noise source.

2.2. Atmospherics

2.2.1. Different kinds of sferics

Atmospherics are defined as the radio noises originated in the natural phenomena occurring within the atmosphere, and the most important noise source for atmospherics is considered to be lightning discharges. However, we can list other possible sources of sferics due to the similar natural electrical disturbances as follows; (1) electrified droplets, (2) dust, (3) blizzard, (4) volcano eruption. Then, we call these collectively "precipitation statics". The atmospherics can be roughly classified into the two types; (1) "stationary sferics" whose intensity and direction of arrival exhibit approximately the same diurnal pattern and whose seasonal variation is also very small. The other is "drifting atmospherics" due to the local thunderstorms, typhoons etc.

2.2.2. Generation sources of atmospherics

It has been established that the average frequency of lightnings over the Earth is about 100-400 flashes every second, originated from about 1000 storms. Each storm covers a certain range of the surface of the order of 20-200 km² (about 16% of the Earth's surface in total), and moves with a speed of 30-50 km/h. Above the land the storm activity takes place mostly during the summer in the local time of 13 to 15h, while above the sea it occurs during the winter in the night and morning hours, usually lasting 1 to 2 hours.

One of the simplest way to describe the storm activity in a specific region is by giving the so-called "number of stormy days". The day is counted as being stormy if at least one instance of thunder is registered within the reach of the observation point (~20km). An example of the world-wide map illustrating the number of stormy days in a year is shown in Fig.2.2-1 (a). The storm activity at different geographic regions exhibit different properties. In the area situated above 82°N and 60°S, and also in the desert areas, storms with electric discharges are generally not observed. The areas for which the number of stormy days exceeds 100, are called "world storm centers", and we find such centers in Africa, South America, and South-East Asia. The number of stormy days in a year is, however, not a precise indicator, because the meteorological observatory network is not dense enough and not uniform.

A more precise characteristic quantity to define the storm activity is the number of discharges per specified area in a particular period of time, which is determined by radio methods. The map illustrating the distribution of the number of storm discharges per 100km² per year is shown in Fig.2.2-1(b). The world storm centers are again identified in this figure and the distribution in Fig.2.2-1(b) is considered to be very similar to that in Fig.2.2-1(a).

Atmospheric radio noise originates in thunderstorms throughout the world, and it varies over a wide range as a function of a number of parameters such as the geographical location, radio frequency, time of day and season. Some of these variations are systematic, while others are random and require a statistical description. The observations of atmospheric noise are conducted systematically at several stations in the world. In the following sections we indicate more detailed characteristics of atmospherics.

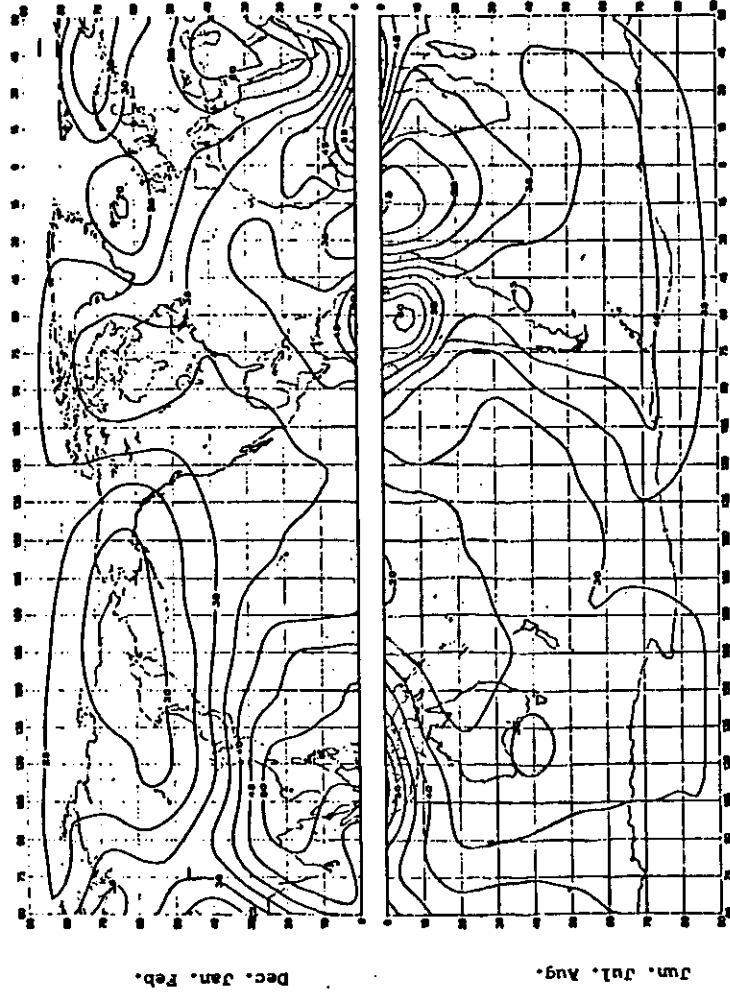


Fig.2.2-3 Expected values of atmospheric radio noise, F_{am} (dB above KT_0 at 1MHz)
(Winter; 0800-1200 LT)

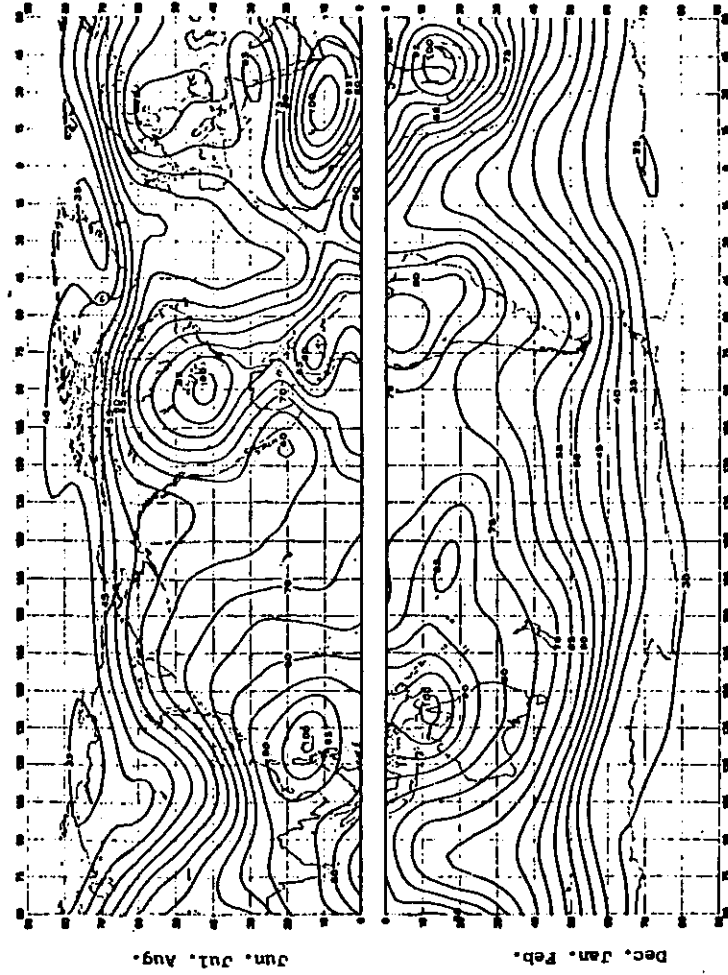


Fig.2.2-4 Expected values of atmospheric radio noise, F_{am} (dB above KT_0 at 1MHz)
(Summer; 0000-0400 LT)

time transitions are noted by the vertical dashed lines. In the radio bands above the ionospheric cutoff frequency, observed atmospheric noise is of local origin, arising from lightning discharges associated with thunderstorm activity occurring within line-of-sight range of the observing point (drifting sferics).

Figs. 2.2-3 and 2.2-4 are the illustrations of the corresponding world-wide distribution maps of atmospheric radio noise intensity given as the median noise figure (F_m) for different seasons of the year and for different times of the day so that we can understand the seasonal variation of the intensity of atmospheric radio noises.

2.2.4. Frequency spectrum of atmospherics

The atmospheric noise intensity varies with frequency, because the electromagnetic energy emitted during a storm as well as its attenuation on the propagation path, are frequency dependent. The geographical dependence is such that the highest levels are observed in equatorial areas and the lowest in polar areas as described in 2.2.2. The noise level is also dependent on the local topography of the terrain. Fig. 2.2-5 illustrates the frequency dependence of atmospheric radio noise intensity, and it implies that the noise intensity, generally, decreases with increasing frequency. Being associated with the temporal variation of the ionospheric effect on radio wave propagation, the frequency dependence of atmospheric radio noises varies correspondingly with L.T. For the drifting, nonstationary atmospherics in the frequency ranges, 0.3-5 MHz and 10-20 MHz, the intensity of atmospherics, E is given by the following relationship (a_1, a_2 : constants).

$$E = a_1 f^{-1} \text{ (night)} \\ = a_2 f^{-2} \text{ (day)}$$

Also, it is statistically known that for a group of atmospherics in the long wavelength (VLF, LF) their intensity E and their occurrence number N [no/sec] are related by,

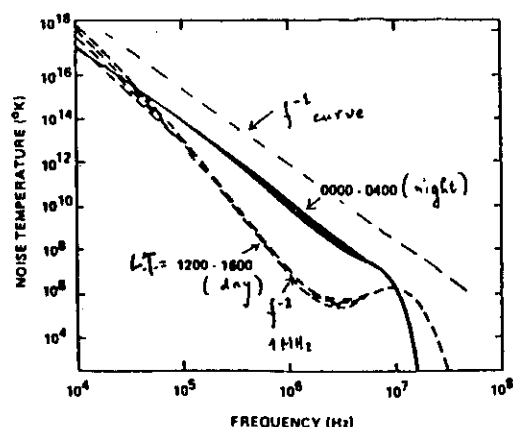


Fig. 2.2-5 Frequency dependence of atmospheric radio noises for the night and day conditions.

$$N E^2 = K$$

where K is a constant.

The sferics in the broadcasting frequency range exhibit a more conspicuous diurnal variation than that in the frequency range of long waves by comparing Fig. 2.2-5 with Fig. 2.2-2, such that their intensity is enhanced from sunset to sunrise and very weak during daytime.

The radio noise in the short wave range increases by about 30 dB due to the nearby lightnings located within 30 km from the observer, but the lightnings located more than 80 km from the observer have no influence on the level of stationary sferics.

The radio noise at the frequency above 50 MHz in the very short wave range, are considered to be entirely due to the drifting sferics, and their intensity E [$\mu V/m$] shows the following dependence on the distance d [km].

$$E = c_1 d^{-1} \quad (d < \sim 30 \text{ km}) \\ E = c_2 d^{-2} \quad (d > \sim 30 \text{ km})$$

where c_1 and c_2 are constants. Then, there are extremely few reports on the sferics in the SHF (cm waves).

2.2.5. The waveforms of atmospherics

The waveforms of atmospherics can be classified in terms of the difference in generation mechanism. The "main discharge stroke type" is a waveform of a damped oscillation associated with ground discharges, as shown in Fig. 2.2-6, which is characterized by the tendency of the period to be larger for decreasing amplitude. The "multiple stroke type" stands for a phenomenon of multiple discharges along the same lightning channel with a period of 5-50 ms, and it is considered roughly as a succession of the main stroke types. The "leader stroke type" is relatively weak in intensity, and it contains mainly higher frequency components as shown in Fig. 2.2-7. It takes place during the step-type discharges preceding the main stroke. The "intracloud discharge type" is considered to be due to the discharge between intraclouds, and its waveform is just like a differentiation of several step-like waveforms, which are occasionally accompanied by damped oscillations with short periods (see Fig. 2.2-8). Then, the "ionospheric reflection type" takes a waveform similar to the main stroke type, due to the multiple reflections from the ionosphere even for one stroke. This type is only observed during nighttime. The summary of the characteristics of different types of atmospherics is given in Table 2.2-1.

2.2.6. Statistical properties of atmospherics

The intensity of atmospheric radio noises is usually determined at the output of a band-pass filter transmitting only a narrow frequency band of its whole spectrum. Whenever the bandpass of the filter is a small fraction of the center frequency ω_c , a narrowband process $n(t)$ results and it means that the received noise is describable in terms of its envelope $v(t)$ and phase $\phi(t)$.

$$n(t) = v(t) \cos[\omega_c(t) + \phi(t)]$$

The phase $\phi(t)$ is uniformly distributed and is usually of secondary significance. The envelope of the process $v(t)$ may be described by several parameters; (1) amplitude probability distribution (APD), (2) crossing rate distribution (CRD), (3) pulse width distribution (PWD), and (4) pulse spacing distribution (PSD) and so on. Detailed description of the statistical treatment of random noises will be given in Section 6.

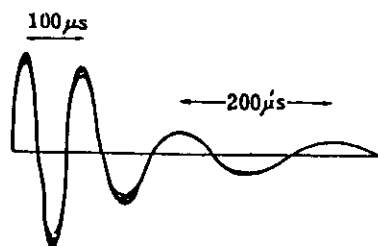


Fig.2.2-6 Waveform of atmospherics of main stroke type

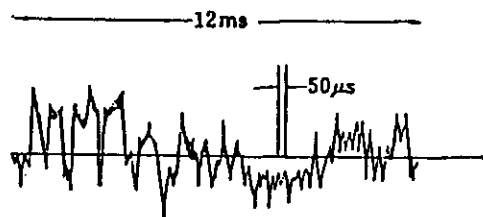


Fig.2.2-7 Waveform of atmospherics of leader stroke type

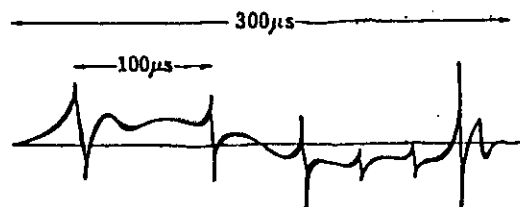


Fig.2.2-8 Waveform of atmospherics of intracloud discharge type

Table 2.2-1 Characteristics of different waveforms of atmospherics

Type of waveform	Duration of one stroke	Total duration	Interval of occurrence	Number of occurrence	Period	Frequency	Discharge current
Main stroke type	165 μs (50-240)	600 μs (100-3,000)	20 ms (6-30)		180 μs (70-300) 130 μs (50-300) 13 μs (10-20)	5.5 kHz (3-15) 7.5 kHz (3-20) 75 kHz (5-100)	20 kA (10-100)
Multiple stroke type		462 ms (ground discharge) 542 ms (intracloud discharge)	35 ms (0.6-180) 70 ms (1.2-253)	11 (2-27)	Same as above	Same as above	Same as above
Leader stroke type	5 ms (1-15)	12 ms (1-60)			200 μs (100-1,000) 50 μs (40-65) 30 μs (5-50)	5 kHz (1-10) 20 kHz (15-25) 30 kHz (20-200)	5 kA
Intracloud discharge type	300 μs (100-1,000)	10 ms (5-15)	1 ms (0.5-5)	2 (1-13)	100 μs (30-240)	10 kHz (4-30)	
Ionospheric reflection type		3 ms (0.5-5)			400 μs (300-500)	2.5 kHz (2-3)	

The APD is most commonly used, which is defined as the fraction of the total measurement time, T for which the envelope is above a level v_i

$$D(v_i) = \text{Prob} [v \geq v_i] = 1 - P(v_i)$$

where $P(v)$ is the cumulative distribution function, $P(v) = \int_0^v p(x) dx$ ($p(x)$, probability density function). Examples of the amplitude probability distributions of atmospheric radio noises are presented in Figs. 2.2-9 and 2.2-10. These results are plotted in the coordinate system in which the Rayleigh distribution, corresponding to the Gaussian thermal noise, is represented by a straight line with a slope equal to -2. For the Gaussian thermal noise, the cumulative probability distribution $P(v)$ is given by

$$P(v) = \exp\left(-\frac{v^2}{2\psi^2}\right)$$

This is the Rayleigh distribution determined by a single parameter ψ . The effective and mean values of the envelope of noise of this kind are correspondingly,

$$v_{\text{eff}} = \lim_{T \rightarrow \infty} \left[\frac{1}{T} \int_0^T v(t)^2 dt \right]^{1/2} = \sqrt{2} \psi$$

$$v_{\text{mean}} = \lim_{T \rightarrow \infty} \left[\frac{1}{T} \int_0^T v(t) dt \right] = \frac{\sqrt{\pi}}{2} \psi$$

As is shown in the figures, for low levels of atmospheric noise its distribution is approximated by this Rayleigh distribution. A deviation from this distribution indicates a domination of individual impulses, and it is observed at higher amplitude levels of the envelope. In this range the empirical distribution is approximated by a log-normal distribution as given in Fig. 2.2-11. The probability density function $p(v)$ for the log-normal distribution is given by the following equation.

$$p(v) = \frac{1}{\sigma \sqrt{2\pi} v} e^{-\frac{1}{2} \left(\frac{\log v - v_m}{\sigma} \right)^2}$$

where v_m is the median value and σ is the standard deviation of $\log v$. This log-normal distribution gave reasonable approximations to the impulsive tail of the distribution, but did not match the Rayleigh (Gaussian) character of the interference at lower amplitude levels, which can be easily expected from Fig. 2.2-11.

For a given period of the day and the season of the year, the variations of atmospheric noise level have a random character and difficult to predict. However, we can describe them statistically. If the probability of the average hourly variations (so-called time block) is plotted in the log-normal coordinates as shown in Fig. 2.2-12, we can approximate it with two straight -line segments. Thus, the variations around the average values are characterized by two parameters D_0 and D_1 defined in Fig. 2.2-12. D_0 and D_1 are the upper and lower decile values, i.e. the values exceeding 10% and 90% of the time. Figs. 2.2-13 and 2.2-14 represent noise variability and character as a function of frequency for the data corresponding to Figs. 2.2-3 and 2.2-4, respectively.

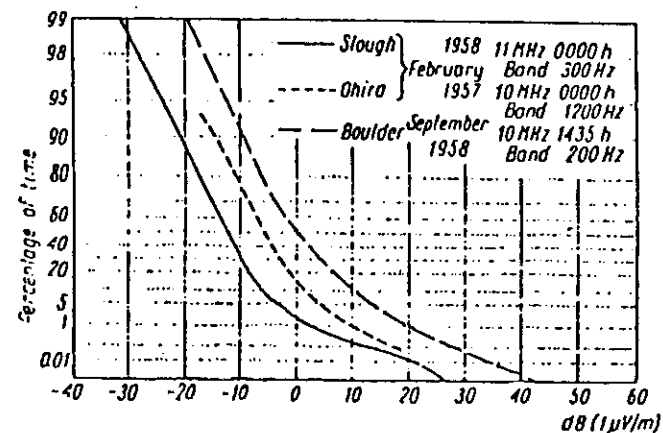


Fig. 2.2-9 An example of amplitude probability distribution (APD)

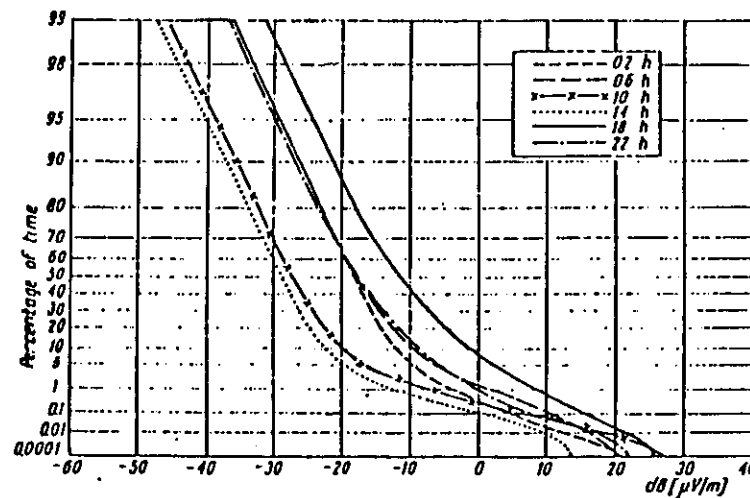


Fig. 2.2-10 Example of diurnal variations of amplitude probability distributions. Slough, 11 MHz, August 1958.

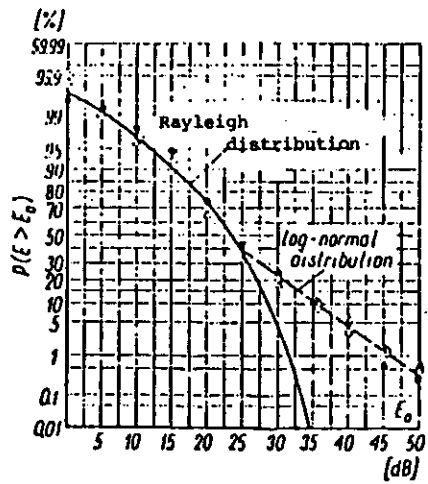


Fig.2.2-11 An example of APD of atmospheric radio noises. Ohira(Japan), 10 MHz, July 30 1966.

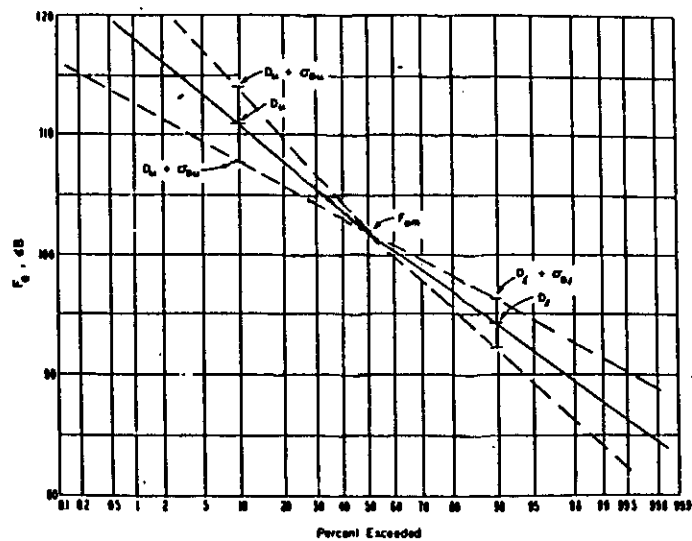


Fig.2.2-12 The distribution of F_a values expected at Boulder, Colo., 500 kHz. Summer season, 2000-2400 hr.

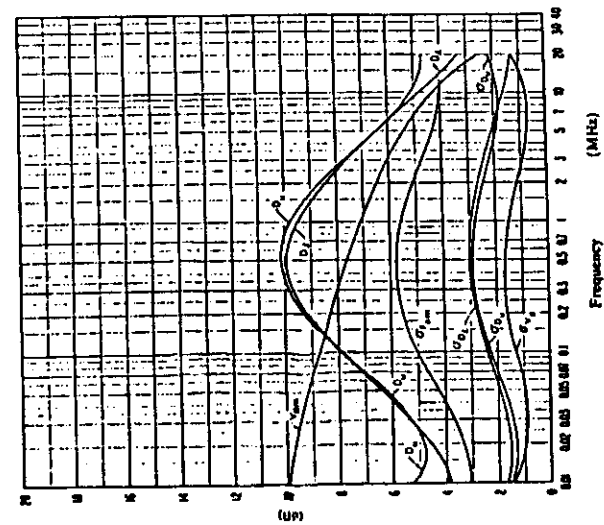


Fig.2.2-14 Data on noise variability and character. Summer, 0000-0400 LT.

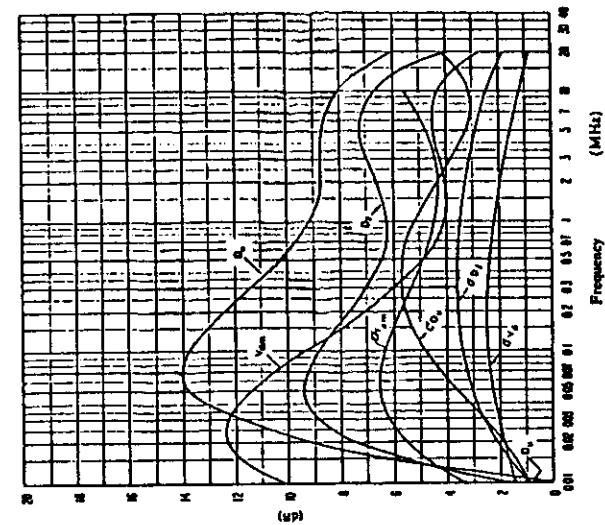


Fig.2.2-13 Data on noise variability and character. Winter, 0800-1200LT. G_{Fam} ; standard deviation of values of F_{am} , D_1 ; ratio of G_{Fam} upper decile to median value, F_{am} , G_{D_1} ; standard deviation of D_1 , D_1 ; ratio of median value, F_{am} to lower decile, G_{D_1} ; standard deviation of D_1 , V_{dm} ; expected value of median deviation of average voltage. The values are for a bandwidth of 200Hz, G_{Vd} ; standard deviation of V_d .

2.3. Radio noises of extra-terrestrial origin

2.3.1. General information

Noises from sources external to the Earth, may be more important than atmospheric noises, which can be understood from Fig.2.1-1. The sun and other members of the solar system contribute part of the extra-terrestrial background, and the remaining cosmic noise has both galactic and extragalactic components, being important at VHF. These radio noises are becoming important because of the development of space communication via satellites. From the standpoint of space communications in the VHF band above 20 MHz, two important noise sources are galactic and solar noises. Since these noises are coming from the sky, the directivity of receiving antenna makes it possible to avoid these noises except in the case of space communications. In the following subsections, we provide a more detailed description of the characteristics of different extra-terrestrial radio noises.

Extraterrestrial radio noise intensity is often expressed in terms of the equivalent radio emission temperature, which is defined as follows. The radio source is assumed to be a black body at a temperature T [°K], and we express the amount of electromagnetic energy from the body passing through a unit area [lm^2] perpendicular to the propagation direction, in a unit time [s] and in a unit solid angle as $d\Omega$ [W]. Then, we have the following expression.

$$dW = \frac{2 \kappa T}{\lambda^2} B d\Omega$$

Here λ is the wavelength [m], B , the frequency bandwidth [Hz] and $d\Omega$ is the solid angle element. This is again the Rayleigh-Jeans' law. This T is the equivalent radio emission temperature.

A perfect black body radiates (and absorbs) ideally electromagnetic waves of all frequencies and at every temperature, and its radiation intensity depends entirely on the temperature and frequency (wavelength). In the radio frequency range the black body radiation is known to follow the Rayleigh-Jeans law. While, at higher frequencies (generally at $hf \gg \kappa T$, h ; Planck constant) Planck's law is valid, the Rayleigh-Jeans formula taking its asymptotic form.

2.3.2. Galactic and cosmic radio noise

An illustrative radio map of the whole sky is presented in Fig.2.3-1, which indicates the results obtained at a frequency of 150 MHz with a resolution of $2^\circ \times 2^\circ$. The emission sources are distributed over the whole map (but not uniformly), and a concentration is noticed in the vicinity of the galactic plane, this fact being observed at all frequencies. The galactic noise is generated within our galaxy by numerous unresolved, discrete sources plus a continuum emission concentrated in the plane of the galactic equator.

The frequency spectrum of galactic noises is shown in Fig.2.3-2 in the frequency range from 1 to 100 MHz as being appropriate for vertical half-wave dipoles near the surface of the Earth. The curve exhibits a frequency dependence of $f^{-2.3}$ and the noise temperature is very high for decametric and metric waves (HF, VHF).

In the frequency range of 10 GHz or above, galactic noise becomes negligible compared with a residual noise which is interpreted today as being of cosmic origin. This noise seems to be isotropic and to have the spectrum of a black body with a temperature of 2.76°K.

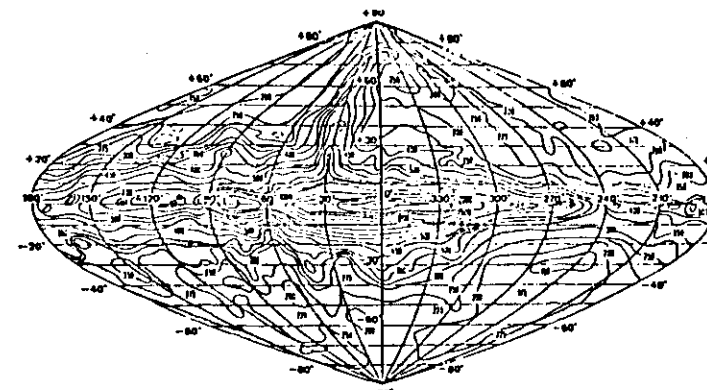


Fig.2.3-1 Examples of galactic noise chart: 150MHz sky brightness in galactic coordinates.

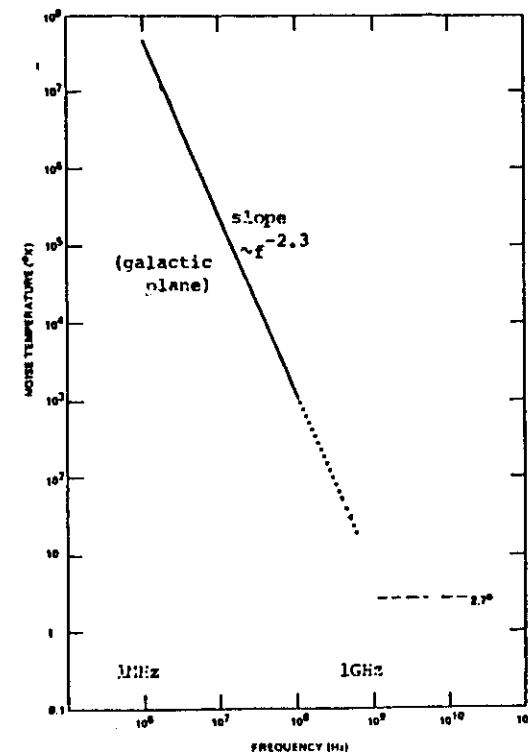


Fig.2.3-2 Frequency dependence of cosmic noise temperature.

2.3.3. Discrete radio sources

This term generally covers all objects of apparently small dimensions which are sources of detectable radio transmissions. These radio sources correspond to very different types of objects in the sky; supernova galactic gas clouds, galaxies, quasars, etc. (Cassiopeia A is the remnants of a supernova which exploded in 1750). The spectrum is generally non-thermal, i.e. the spectral noise density does not correspond to that of a black body at a fixed temperature. Two strong radio sources among them are Cassiopeia A and Cygnus A. The frequency dependence of their power flux density is illustrated in Fig.2.3-3, together with other sources such as quiet sun, active sun, galactic noise and moon.

2.3.4. Radio noises from the solar system

Solar radio emissions are classified roughly into the following three types according to their generation mechanism, and these three types are summarized in Fig.2.3-4. The first type is the quiet sun radiation, which is the constant component of solar radiation and is the black body radiation. The second type is the component that displays long-term variation, being connected with variations in number of sunspots and it is frequently observed at a particular wavelength range from 3cm to 60 cm. The last type arises from isolated radio flares or radio bursts.

The quiet-sun radiation produces power flux spectral densities on the Earth which increases with frequency as indicated in Table 2.3-1 and Fig.2.3-4 (also in Figs.2.3-3 and 2.1-1). This radiation is observed over a wide range from millimeters to meters. Its intensity is determined during periods of minimum solar activity and it corresponds to an effective temperature, changing from 6×10^3 °K for the millimeter waves to 10^6 °K for the meter waves. The second radiation component displays slow variations with a noticeable 27 day cycle, and it is identified with the correlation with the number of sunspots. Its intensity on the wave range 3-50 cm is three times higher than the radiation background. The final solar-flare radiations vary in spectral content, duration and polarization. While the black-body radiation is randomly polarized, the radio bursts are known to be circularly polarized. The rise in noise level lasts for a few minutes and on some occasions of severe disturbances, the succession of radio bursts endures for a few days. Solar-flare radiations are classified by their features into five flare types as given in Fig.2.3-5. The radio spectrum for a Type IV flare is shown in Fig.1.4-1 and may be compared with the emission of the quiet sun. The flux density of a Type IV flare is not the largest of the five flare types, but Type IV emissions are broadband and stable, capable of persisting for periods of several days. While, Types I, II and III have been observed to emit greater power densities than Type IV.

Radiations are known to be emitted from the planets. The strongest one is Jovian radiations which are of non-thermal origin due to the high-energy electrons in its magnetosphere. Ionospheric opacity of the Earth's atmosphere produces the apparent extinction at the Earth's surface of the Jovian flux at frequencies below 20 MHz, as given in Table 2.3-1 and Figs.1.4-1 and 2.1-1.

The lunar emission spectra presented in Figs.2.1-1 and 2.3-3, and manifesting a distinct positive slope is that of a black-body whose temperature varies between 100°K and 300°K during the lunar cycle.

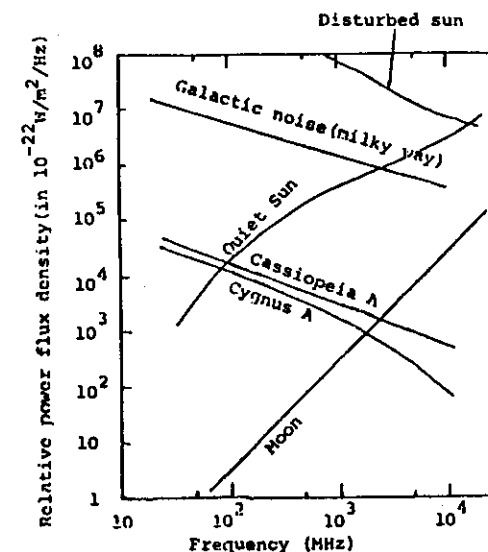


Fig.2.3-3 Frequency dependence of relative power flux density of representative radio sources

Table 2.3-1 Power flux spectral densities from the sun, the moon and Jupiter (in $W m^{-2} Hz^{-1}$).

Source	Frequency (GHz)/Wavelength (m)						
	0.03 10	0.1 3	0.3 1	1 0.3	3 0.1	10 0.03	30 0.01
Solar bursts	$2.8E-17$	$9.1E-18$	$3.0E-18$	$3.7E-18$	$2.7E-18$	$1.2E-18$	$5.3E-19$
Quiet sun	$1.0E-22$	$1.0E-21$	$2.4E-21$	$3.5E-21$	$6.5E-21$	$2.9E-20$	—
Average moon	—	—	$4.4E-25$	$4.6E-24$	$3.9E-23$	$4.4E-22$	$3.6E-21$
Jupiter	$4.0E-26$	$6.3E-26$	$7.9E-26$	$8.5E-26$	$7.4E-26$	$1.7E-25$	$1.8E-24$

$$e-n = 10^{-n}$$

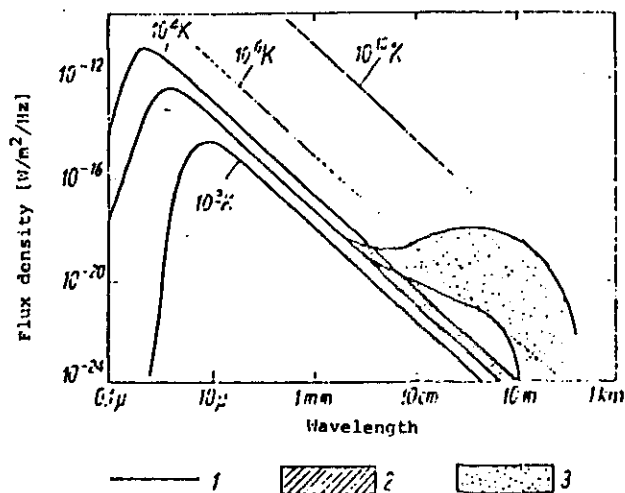


Fig.2.3-4 The solar emission spectrum and the black body spectrum for various temperatures. 1- Thermal emission, 2- Non-thermal emission from the quiet sun, and 3- Non-thermal emission from the active sun.

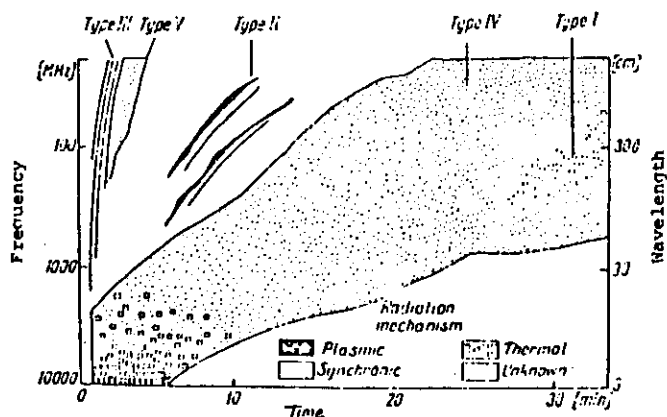


Fig.2.3-5 Dynamic characteristics of solar radio emission burst. Time elapsed since the beginning of the flare.

3. Man-made noise

3.1. General description

The natural electromagnetic processes discussed above are originated in the universe and constitute fundamental elements of the Earth's environment. Relatively recently, however, man began introducing new elements into this environment, and they are man-made noises due to the human activity. These man-made noises are the external noises generated by the traffic systems, power transmission lines and the electrical equipments connected these power lines, and hence these noises are sometimes called "industrial noises".

Just like the atmospheric are roughly divided into two major groups, (1) stationary ones and (2) non-stationary, drifting ones, man-made noises are also classified into three types depending on the magnitude and nature of the noise sources:

(1) City (industrial) noise:

Even if there are no specific nearby man-made noise sources, we encounter the interference as the composite of many noise sources in the distant, in the rural region of high pollution (we call this "city noise"). In this case, it is of no importance to consider the waveforms of individual noises and their generation mechanism, and its magnitude is roughly proportional to the cultural activity utilizing the electricity. Also, as the consequence of the composite of many noise sources, there is no specific polarization and it is considered to be continuous noise.

(2) Building noise:

This building noise is the radio interference taking place in the telecommunication or radio wave reception at the different places such as the power generating point, telecommunication stations, factories, big buildings, ships and so on. While the city noise gives the interference through aerials, the building noises come on many occasions on the feeding lines between the aerials and the receivers. It is rare that this noise is continuous.

(3) Single man-made noise source:

We have noises generated from the discharge noise from particular electrical equipments, corona noises from specific transmission lines and so on, and it is defined as the noise from a single electric equipment, with possessing its specific waveform and intensity. The degree of interference is dependent on the surrounding condition and this noise belongs to impulsive noise. The range of interference from individual noise source is considered to be limited by $\lambda/2\pi$.

The macroscopic observation of man-made noises provides useful information on the city noise (1) as the composite noise, and the microscopic measurement refers to the noise category (3). Noise category (2) is the intermediate of the two types (1) and (3). The intensity of city noise (1) is a function of time, frequency and measuring location, and it is closely correlated with the electrical power consumption, which indicates indirectly that the city noise (1) is related with the population and cultural activity of the urban region.

3.2. Sources of man-made noises

3.2.1. Unintentional man-made noise and intended coherent radiation

There are many devices emitting electromagnetic energy, and one can divide them into two groups. The first includes devices built especially for the purpose of radiating energy, and the second includes those in which this radiation constitutes "unintentional noises".

Radio transmitting devices such as television, radio communication, radio navigation, radar etc belong to the first group. Their unit powers can differ a great deal and sometimes reach up to 10 MW. In addition to their desired emissions, such powerful transmitters can radiate broadband noise, harmonics, and other unintentional radiation, and they cause problems to nearby receivers.

Unintentional man-made radiators also contribute to the composite electromagnetic environment. Table 3.2-1 summarizes some of the primary categories of such radiators, and it includes superheterodyne radio and TV receivers (local oscillator radiation), automobiles (radiation of the ignition system), various electrical devices, appliances with electric motors, lighting devices, neon signs, high voltage power lines, medical

Table 3.2-1 Categories of unintentional radiators

Overhead power transmission and distribution lines
Ignition systems (e.g., automotive, aircraft, small engines, etc.)
Industrial fabrication and processing equipment (including arc welders)
Electric motors and generators
Electric buses and trains (excluding their power lines)
Contact devices (e.g., thermostats, bells, and buzzers)
Electrical control, switchings, and converting equipment (e.g., SCRs, and ac/dc converters)
Medical and scientific apparatus
Lamps (e.g., gaseous discharge devices and neon signs)
Various electrical consumer products (including electronic games and computers)

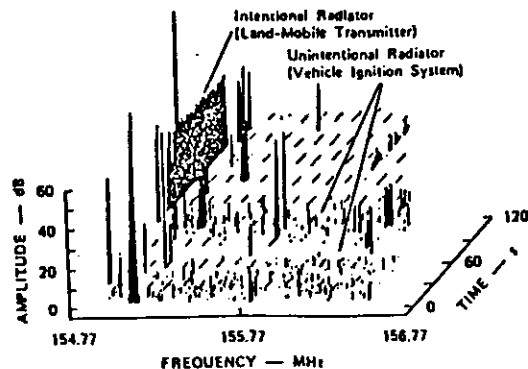


Fig.3.2-1 Examples of contributions to the composite electromagnetic environment by intentional and unintentional radiators.

devices and many others. The level of radiation from these equipments and devices is typically much less than the levels from intentional radiators. Fig.3.2-1 is an example of the relative contributions to the composite noise environment at 155 MHz. We notice, from this figure, the relative significant contributions of the land-mobile transmitters and the ignition noise. In the following, we discuss the properties of two major incidental noise sources, (1) power transport and generation facilities (distribution lines, transmission lines, etc) and (2) automotive sources (ignition circuitry, alternators, generators, electric motors etc).

3.2.2. Radio noise from power transmission and distribution lines

Radio noises arising in electric-power production, conversion and transport facilities occur within the spectral range extending from the fundamental generation frequency (50 or 60 Hz) into the UHF range. Throughout this frequency interval, the radio noise intensity in the immediate vicinity of power transport facilities arises from one or both of the two types of noise sources, "gap breakdown" and "line conductor corona". Either source emission level may be comparable to or greater than the noise levels of other man-made sources. Furthermore, the resulting radiation may exceed atmospheric noise levels between sunrise and sunset when the daytime noise minimum occurs, which in mid-latitudes represents a decrease of 20 dB from the diurnal maxima evident in the middle and lower portion of the HF band (Fig. 3.2-2). Levels of incidental radiated noise comparable to those observed on transmission and distribution lines and arising from incidental cause originate from power-conversion facilities such as local transformer substations.

Overhead power line noises are important mainly below 15 to 20 MHz, as given in Fig.3.2-2. Power lines can be categorized by their function, which determines their operational voltage and noise-generating mechanism. The lower-voltage distribution and transmission lines (below about 70 kV) produce noises from various types of discharges in gaps, while the high-voltage transmission lines (110 kV and higher) generate noise by various kinds of corona. The high rate of current rise transforms to a broader spectrum for gap noise than for corona noise, as observed with peak detectors and with quasi-peak detectors (see Fig.3.2-2). The low-voltage lines may also radiate noises resulting from switching transients and other effects and from devices connected to the lines.

High-voltage DC transmission lines are coming into use. It is pointed out that the noise is generated at the conversion stations, which then propagates on the lines.

The noise from power lines is greatly influenced by the weather and by the state of maintenance of the line. Fig.3.2-3 illustrates the median values of average noise power spectral density data obtained in the near field at MF, HF and VHF with rms detectors. Vertical monopole antennas are used, directly under the line. The figure shows that at any given frequency the difference between measured medians for the noisiest and the quietest line was about 30 dB for these fair-weather data. Noise increases of 17 dB are likely during rain and we expect more enhanced noise during snow. Also, in about 60% of the measurements, those made with horizontally polarized dipoles produce greater noise than those made with vertically polarized dipoles. The differences range from 0 to 10 dB over the frequency range band 15 kHz to 10 GHz.

Fig.3.2-4 presents examples of APDs for a 115-kV transmission line for which we expect the largest noise power in Fig.3.2-2. Also, we can study the variation of APD with the weather condition.

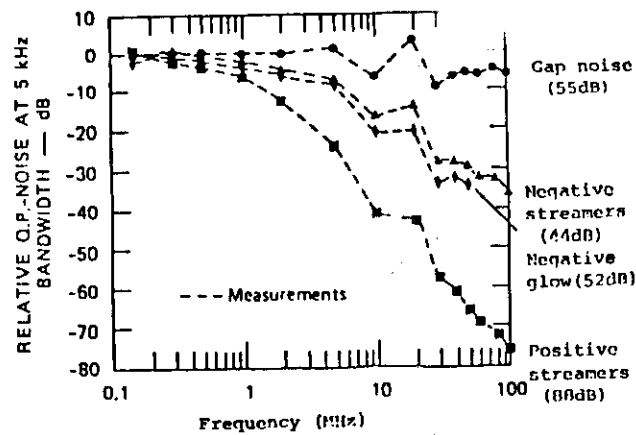


Fig.3.2-2 Relative frequency spectra for different power noise types. The numbers in parentheses are the absolute values measured at 0.150 MHz.

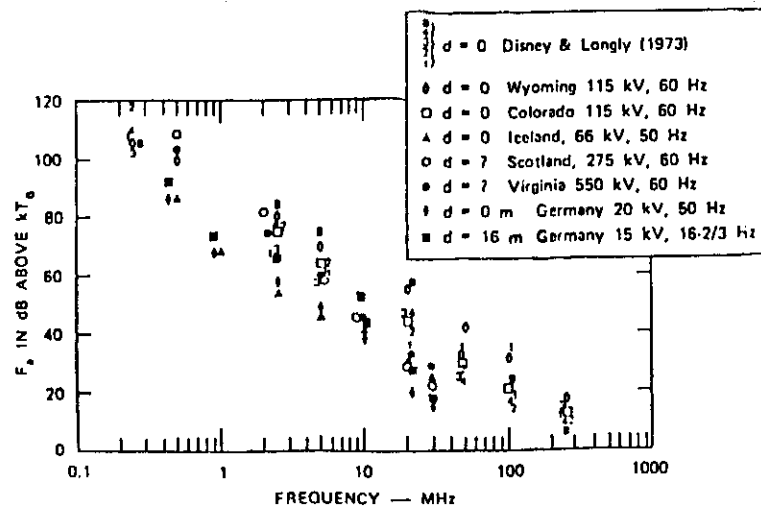


Fig.3.2-3 Average noise power approximately underneath selected power lines.

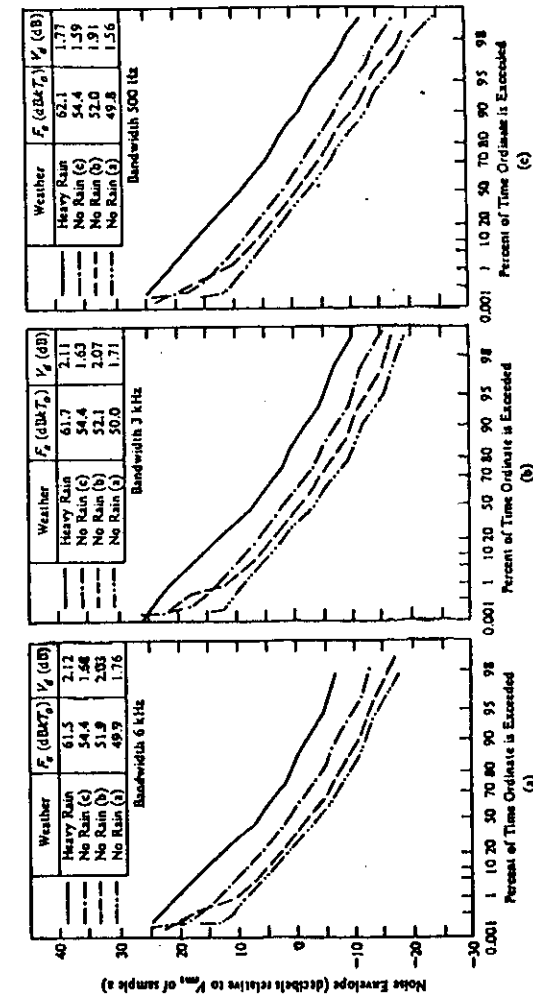


Fig.3.2-4 APDs (corona noise) for three conditions of dry line and one of heavy rain as measured at 3 MHz for a 115-kV AC transmission line. Test site was laterally displaced 50 ft from the line center. F_p and V_p are noted for each weather condition and each of three values of detector bandwidth of 0.5, 3 and 6 kHz.

3.2.3. Automotive noise

Ignition noise is generally found wherever automobiles or other vehicles using spark-initiated power systems are used. The sources of ignition noise include the distributor, spark plugs and generator. Typically in a given frequency band, one of these is the dominant source. This noise is highly impulsive and spreads over much of the frequency spectrum. At the low end of the spectrum (below about 20MHz), ignition noise is generally believed to be exceeded by power line noise when both sources are present. The actual lower limit will be determined by specific situations, including the density of automobile traffic and the proximity of power lines. The high frequency limit to the automobile ignition noise spectrum has not been as well studied.

The APDs of three vehicles measured in an 8 kHz bandwidth are shown in Fig.3.2-5, and we note the change in the shape of APDs in the figure as a function of engine speed. The sharp increase in negative slope beginning at abscissa values of up to 5 percent is a dramatic manifestation of the impulsive character of ignition-system noise. Fig.3.2-6 gives the time statistics of the peak envelope, in which the peak-envelope values exceeded for varying percentages of the 15-min observation period are given. This figure indicates that the automobile noise increases in intensity with frequency above 30 MHz and exhibits a relatively flat spectrum above 100MHz, giving interference to televisions. Fig.3.2-7 indicates a good correlation of the noise intensity with the automobile density, as measured at 100 MHz.

3.3. Composite city noise

With a high number of sources operating simultaneously, the resulting process consists of dominant singular components of particularly high intensity and of background electromagnetic noise. The discrete components originate from the closest or extremely powerful sources as discussed in the previous sections, while the background noise results from the remaining mass of sources. The most reliable data on the urban electromagnetic environment can be obtained experimentally. Current information is not available for estimating man-made noise intensity under all conditions. But it is possible to derive typical values from limited observations.

The experimental data are presented in Fig.3.3-1, which were based on the measurements made in USA. The results are classified into four groups (A, B, C and D) corresponding to midtown (A), suburban (B), and rural (C) regions, with a separate group (D) containing the lowest observed levels. An indication of the variations encountered from location to location shown in the figure is given by the standard deviation. This parameter has no clear dependence on frequency: The observed data are consistent with the standard deviation equal to about 7dB in all areas. It should be noted that it is not evident that the values shown in Fig.3.3-1 can be applied without reservations to the regions other than those investigated, although the tendency will be valid.

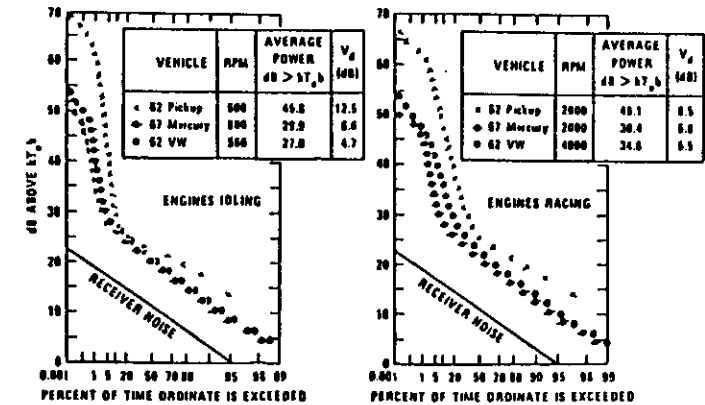


Fig.3.2-5 APDs of radio noises of three different vehicles. Right side at 10n, 24.11 MHz (8kHz noise bandwidth).

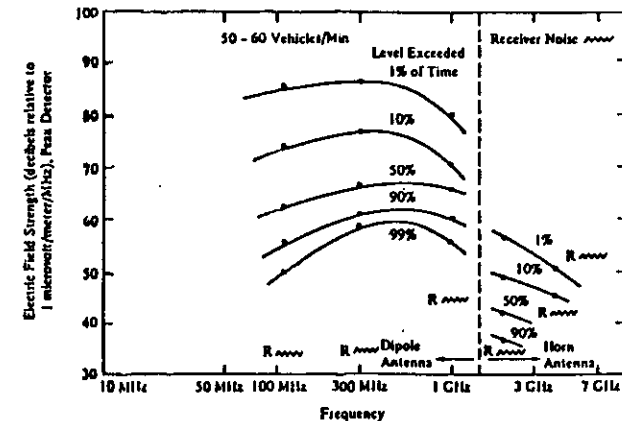


Fig.3.2-6 Peak envelope distributions for automobile traffic noise (15 min sample) as a function of frequency. Observing antenna types: dipole 1GHz and below, horn above 1GHz. Noise bandwidth, 300kHz.

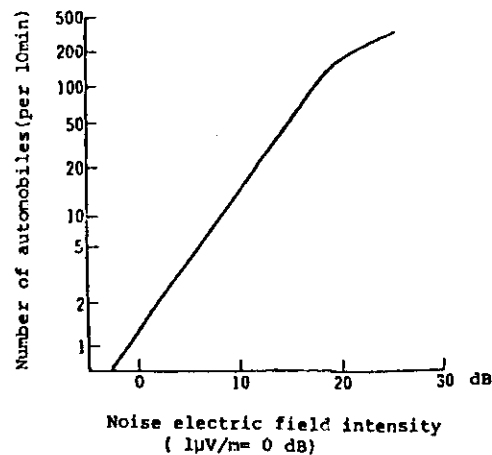


Fig.3.2-7 The correlation between the noise intensity and the traffic density. The noise intensity is measured by the quasi-peak value exceeding 5% of 10 min observational interval. 100 MHz (bandwidth, 4kHz)

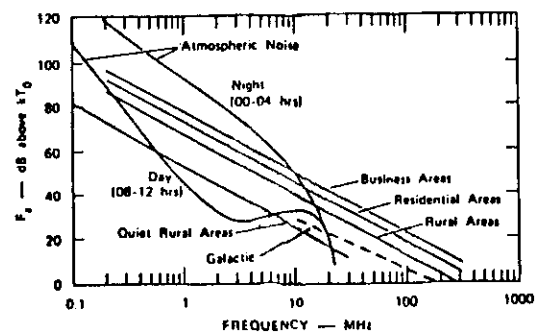


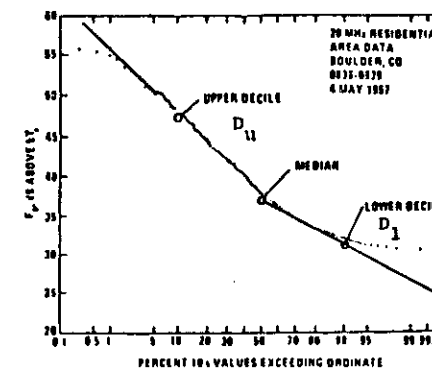
Fig.3.3-1 Estimates of median values of man-made noise power measured by a short vertical lossless grounded monopole antenna. Four different areas are considered. For the sake of comparison, atmospheric noise and galactic noise are plotted.

Table 3.3-1 gives a measure of the time variations within an hour about the hourly median value of noise power at a specific location. Upper and lower decile values D_U and D_L are indicated for several selected frequencies. The definition of D_U and D_L are given in the bottom figure of Table 3.3-1.

When assessing noise influencing a receiver, the gain, polarization and directional properties of the receiving antenna should be taken into account. Fig.3.3-1 concerns an omnidirectional, short, lossless, vertical

Table 3.3-1 Representative upper and lower deciles, D_U and D_L , respectively of noise level variability within an hour at a given location. The definition of D_U and D_L are given in the bottom figure.

Frequency MHz	Business Area		Residential Area		Rural Area	
	D_U (dB)	D_L (dB)	D_U (dB)	D_L (dB)	D_U (dB)	D_L (dB)
0.25	8.1	6.1	9.3	5.0	10.6	2.8
0.5	12.6	8.0	12.3	4.9	12.3	4.0
1.0	9.8	4.0	10.0	4.4	9.2	6.6
2.5	11.9	9.5	10.1	6.2	10.1	5.1
5	11.0	6.2	10.0	5.7	5.9	7.5
10	10.9	4.2	8.4	5.0	9.0	4.0
20	10.5	7.6	10.6	6.5	7.8	5.5
48	13.1	8.1	12.3	7.1	5.3	1.8
102	11.9	5.7	12.5	4.8	10.5	3.1
250	6.7	3.2	6.9	1.8	3.5	0.8



grounded monopole antenna. The values shown in this figure can be easily transformed into rms values of the field intensity E . Geographical variations of man-made noise depend on the spatial distribution of the emission sources. Below about 10 MHz man-made noise is related primarily with the density of electrical devices and electric power lines. This means that they are correlated with the population density, industrial activity and electrical energy consumption. Above 20 MHz man-made noise seems to be correlated with the motor vehicle traffic density and urbanization. And, the set noise of the receiver will be important in the TV band.

Urban radio noise depends on many factors such as, for example, geographical location, time, day of the week, season of the year, frequency and direction, etc. Unfortunately, knowledge of these problems is not yet comprehensive, and this is confirmed by the various study programs of different organizations like URSI and CCIR.

The statistical-physical model of the composite electromagnetic environment has been developed. Analytical first-order probability densities and distributions as observed at the output of typical narrow-band receivers of bandwidth Δf_R are obtained for three basic classes of electromagnetic noise. 1. Class A noise: The frequency components of this type are concentrated to a spectral width (Δf_N) that is less than the bandwidth of the narrow-band receiver (Δf_R) ($\Delta f_N < \Delta f_R$). Consequently, the transient responses of the receiver are negligible relative to the steady-state responses caused by an incident wave. 2. Class B noise; The frequency components of this type extend over a spectral range that is greater than Δf_R ($\Delta f_N > \Delta f_R$), which may experience impulse excitation and manifest exponential signal buildup, signal decay and damped oscillation. 3. Class C noise, which is a linear combination of Class A and Class B components.

These models combine statistical and physical structures; the noise sources are assumed to be independently and randomly distributed in space, and they emit arbitrary waveforms randomly in time, so that the basic statistics are Poisson. The emitted waveforms obey appropriate propagation laws and explicitly include the effect of source and receiving antenna patterns, relative Doppler effects, source distribution in space and other geometrical factors. The results are highly non-Gaussian, as would be expected, but they are analytically tractable and canonical (i.e. the form of the probability structures are essentially invariant of the waveform and of kinematic and geometric details). This is strongly true for Class A noise (such as some man-made noise and communication signals), but only moderately so for Class B noise (such as atmospheric noise and automobile ignition noise) whose statistics are more sensitive to the source distribution and propagation laws. Excellent agreement of the statistical-physical model with experiment is found for the relative APDs of both basic Class A and B, as in Fig. 3.3-2. These quantitative models are useful for (1) the assessment of electromagnetic environments from the purpose of spectrum management, (2) the evolution of receiver performance related to the design of optimum receivers for use in these strongly non-Gaussian noise situations, and (3) analytical determination of system performance.

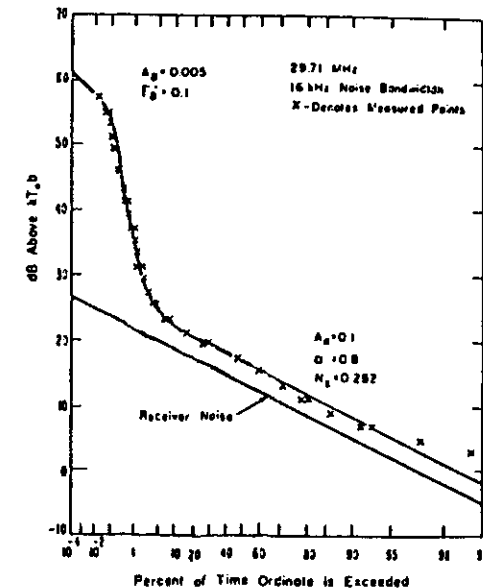


Fig. 3.3-2 Comparison of the measured envelope probability distribution of automotive ignition noise from moving traffic with Class B model.

4. Radio noises and design of radio telecommunication system

4.1. Threshold power at the receiver

For particular modulation/demodulation schemes there exists a certain level of the power P_r at the receiver below which the signal to noise ratio becomes degraded abruptly, but above which we have a significant signal to noise ratio. This level is called "threshold level", and we express P_r at this level as P_{rth} . Then, P_{rth} is given by the following relationship.

$$P_{rth} = \kappa T_0 B \overline{EN}' R \quad [W] \quad (4.1-1)$$

where \overline{EN}' is the effective external noise figure, B is the receiver bandwidth and R is the minimum S/N necessary at the input terminal of the receiver which is dependent on the modulation/demodulation scheme employed. Eq.(4.1-1) is rewritten in dB as follows.

$$P_{rth} = R + B + \overline{EN}' - 204 \quad [dBW] \quad (4.1-2)$$

where R, B, \overline{EN}' are all expressed in dB (e.g. $R = 10 \log_{10} R$ ---). Here, if we assume the propagation loss as L [dB], the minimum necessary transmitting power P_t should be as follows.

$$P_t = L + R + B + \overline{EN}' - 204 \quad [dBW] \quad (4.1-3)$$

As would be expected, L and \overline{EN}' are the values fluctuating temporally and we indicate their median values by L_m and \overline{EN}'_m . Furthermore, in order to maintain a good quality of communication, we are obliged to take into account a surplus power which is called the protection ratio (T_x [dB]), and then the necessary transmitting power P_t will be

$$P_t = L_m + R + B + \overline{EN}'_m - 204 + T_x \quad [dBW] \quad (4.1.4)$$

The accurate estimate of these R and T_x for different kinds of modulation schemes is the aim of the research of the role that radio noises play in radio communication engineering. L_m is connected with the problem of propagation, which is one of the important issues of radio propagation studies. Finally, the study of \overline{EN}' concerns the study of radio noise itself and is the major issue of this lecture.

4.2 Predetection signal to noise ratio and operating noise figure

Since the noise level may result from a combination of noise generated internal to the receiving system and external noise, it is convenient to express the resulting noise by means of the definition of the noise figure of a radio receiver. The system noise factor can be defined in terms of the losses and actual temperatures of the various parts of the system, as illustrated in Fig.4.2-1. Loss in the circuit is taken here to be the ratio of available input power to available output power and will differ from the loss in delivered power unless a matched load is used. The noise factor of the antenna circuit, f_c is

$$f_c = 1 + \frac{T_c}{T_0} (l_c - 1) \quad (4.2-1)$$

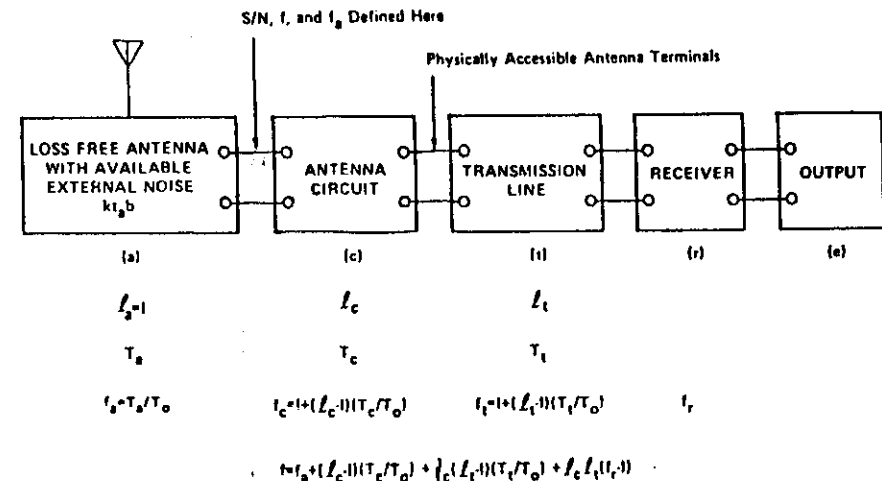


Fig.4.2-1 The receiving system and its operating noise figure, f .

where l_c is the loss factor in the antenna and associated circuit, T_c is the actual temperature of the antenna circuit and nearby ground, and T_0 is the reference temperature (290°K).

Similarly, the transmission line loss factor, l_t , and temperature, T_t , will determine a noise factor, f_t for the transmission line given by

$$f_t = 1 + \frac{T_t}{T_0} (l_t - 1) \quad (4.2-2)$$

Using a receiver noise factor of f_r , and assuming the receiver is free of spurious responses, we can use Friis' method of combining noise figures in cascade to obtain a system noise factor, f including external noise, f_a , which is

$$f = f_a + (l_c - 1) \frac{T_c}{T_0} + l_c (l_t - 1) \frac{T_t}{T_0} + l_c l_t (f_r - 1) \quad (4.2-3)$$

If all temperatures are equal to T_0 , Eq.(4.2-3) becomes

$$f = f_a - 1 + f_c f_t f_r \quad (4.2-4)$$

4.3. Estimates of minimum (and maximum) environmental noise levels

The best available estimates of the minimum expected values of F_a along with other external noise levels of interest are summarized in this section as a function of frequency. Fig.4.3-1 covers the frequency range 0.1 Hz to 10 kHz. The solid curve is the minimum expected values of F_a at the surface of the Earth based on measurements (taking into account all seasons and times of day for the entire Earth), and dashed curve gives the maximum expected values. Note that in this frequency range there is very little seasonal, diurnal, or geographic variation. The larger variability in the 100 to 10,000 Hz range is due to the variability of the Earth-ionosphere waveguide cutoff.

Fig.4.3-2 covers the frequency range 10^4 to 10^8 Hz. The minimum expected noise is shown with solid curves and other noises that could be of interest as dashed curves. For atmospheric noise ($f > 10^4$ Hz), the minimum values expected are taken to be those values exceeded 99.5% of the time, and the maximum values are those exceeded 0.5% of the time. For the atmospheric noise curves, all times of day, seasons, and the entire surface of the Earth have been taken into account. These atmospheric noise data are of average background. Local thunderstorms can cause higher noise levels. The man-made noise (quiet receiving site) is that noise measured at carefully selected quiet sites. The atmospheric noise below this man-made noise level was, of course, not measured, and the levels shown are based on theoretical considerations and engineering judgement. Also shown is the median expected business area man-made noise.

In Fig.4.3-3 the frequency range 10^8 to 10^{11} Hz is treated. Again, the minimum noise is given by solid curves while some other noises of interest are again given by dashed curves. For galactic noise, the average value (over the entire sky) is given by the solid curve labeled galactic noise (Figs.4.3-2 and 4.3-3). Measurements indicate a ± 2 dB variation about this value. The minimum galactic noise (narrowbeam antenna towards galactic pole) is 3 dB below the solid galactic noise curve shown in Fig.4.3-3. The maximum galactic noise for narrowbeam antenna is shown with dashed curve in Fig.4.3-3.

The majority of the results in these figures is for omni-directional vertically polarized antennas (except as noted in the figures). The average value of F_a for directional antennas will be the same if we assume random direction. Studies have indicated that at HF (for example), for atmospheric noise from lightning, there can be as much as 10 dB variation (5 dB above to 5 dB below the average F_a value shown) with direction for very narrowbeam antennas is shown with dashed curve in Fig.4.3-3.

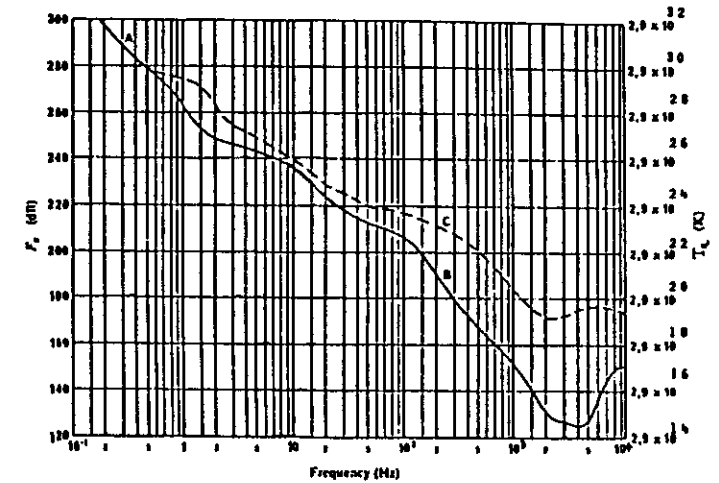


Fig.4.3-1 F_a (minimum and maximum) vs frequency (0.1 to 10^4 Hz). A-micropulsations, B-minimum value expected of atmospheric noise, C-maximum value expected of atmospheric noise.

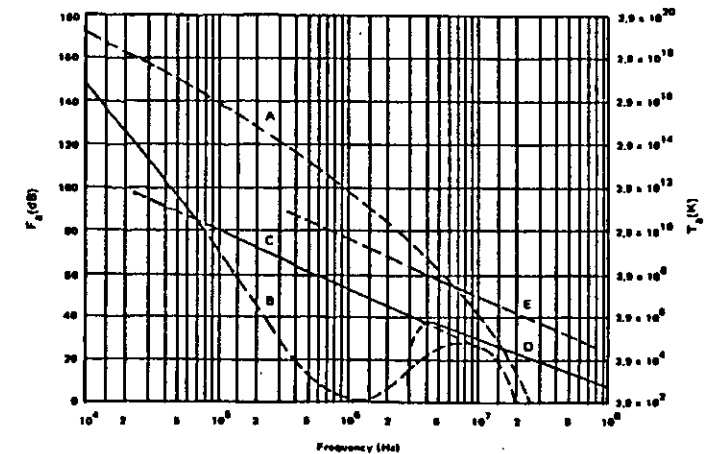


Fig.4.3-2 F_a vs frequency (10^4 to 10^8 Hz). A-atmospheric noise, value exceeded 0.5% of time, B-atmospheric noise, value exceeded 99.5% of time, C-man-made noise, quiet receiving site, D-galactic noise, E-median business area man-made noise; minimum noise level expected.

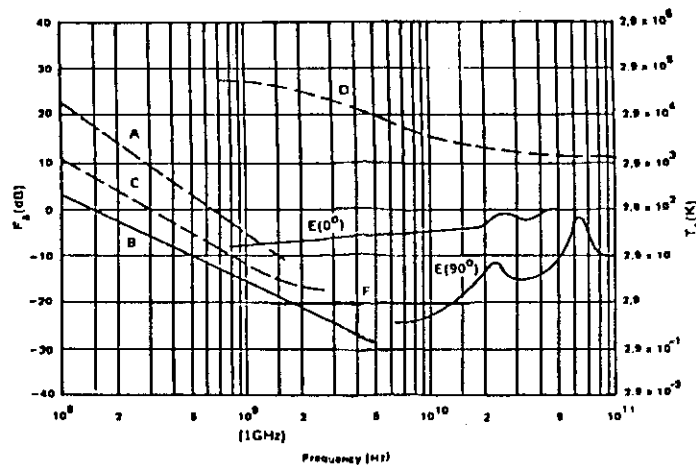


Fig.4.3-3 F_a vs frequency (10^8 to 10^{11} Hz). A-estimated median business area man-made noise, B-galactic noise, C-galactic noise (toward galactic center with infinitely narrow beamwidth), D-quiet sun(1/2 degree beamwidth directed to sun), E-sky noise due to oxygen and water vapor(very narrow beam antenna),upper curve, 0° elevation angle, lower curve, 90° elevation angle, F-black body(cosmic background), 2.7°K , minimum noise level expected.

4.4. Example determination of required receiver noise figure

We now want to consider a simple example to show how to determine the required receiver noise figure. At 10kHz, for example, the minimum external noise is $F_a = 145$ dB(see Fig.4.3-2). If we assume $T_c = T_t = T_0$ and $\ell_c = \ell_t = 1$ (that is, no antenna or transmission line losses), then Eq.(4.2-4) yields

$$f = f_a - 1 + f_r \quad (4.4-1)$$

We can take f_r to be that value which will increase F by only 1dB. This gives us a noise figure, F_r of 140 dB or an overall noise figure, F of 147 dB. Any smaller noise figure, F_r no matter how small, cannot decrease F below 146dB. Consider now that $\ell_c = \ell_t = 100$, i.e. 20 dB antenna losses and 20dB transmission losses. Then,

$$f = f_a - 1 + 10000 f_r \quad (4.4-2)$$

In order to raise the F no more than 1 dB(to 147dB) for the above situation, F_r can only be as large as 100dB. As this example shows, it makes no sense to attempt to use sensitive receivers at low frequencies.

As another example, consider a VHF receiver at 100MHz. The minimum noise level is due to galactic noise and is approximately an F_a of 7 dB. Suppose that $\ell_c = 100$ and $\ell_t = 1$; in order not to raise F more than 1dB, F_r can only be as large as -19.8dB.

In the first example above, the interfering noise was atmospheric noise, and in the second example the noise was galactic. These two types of noise are quite different in character-atmospheric noise being very impulsive and galactic noise being white Gaussian. Correspondingly, these two types of noise will affect system performance quite differently, even if they have the same level (i.e. available power). In specifying system performance, the detailed statistical characteristic of the noise must be taken into account. One consequence of this is that the external noise can still limit performance even though the receiver noise (Gaussian in character) is made as high as possible so as not to increase the overall operating noise factor f . System performance depends on more than noise level, and so far we have considered only noise level via f_a .

5. Internal noise

5.1. Internal noise(receiver internal noise)

There are different kinds of internal noises, which can be classified in Table 5.1-1. These noises (especially the ones classified as "noise" in the table) are mainly due to the atomic nature of matter and electricity, and so they can never be wholly eliminated. These include thermal noise, shot noise and others. In the following, we give a brief description of some representative internal noises.

(a) Circuit noise (thermal noise)

Thermal noise is defined as the fluctuations due to the random thermal motion of the conduction electrons in a resistor, and the thermal-noise voltage generated in a resistance $R [\Omega]$ is given by

$$e_n^2 = 4 k T_0 B R \quad (5.1-1)$$

This equation is identical to Eq.(1.3-3) where $B [\text{Hz}]$ is the bandwidth of measuring system. In the case of a resonance circuit, R is regarded as the resistive component of the resonance impedance, and we take the radiation resistance as R in the case of antennas. If we express Eq. (5.1-1) in dB, we obtain the following equation from the rms value.

$$e_{\text{rms}} = \sqrt{e_n^2} = 126 \sqrt{RB} \times 10^{-12} \text{ [V]} \quad (5.1-2)$$

As shown in Fig.5.1-1, the thermal noise is known to exhibit a flat frequency characteristic over a wide frequency range of our interest, and this kind of noise with a uniform power frequency spectrum, is called "white noise".

(b) Tube, transistor and diode noise

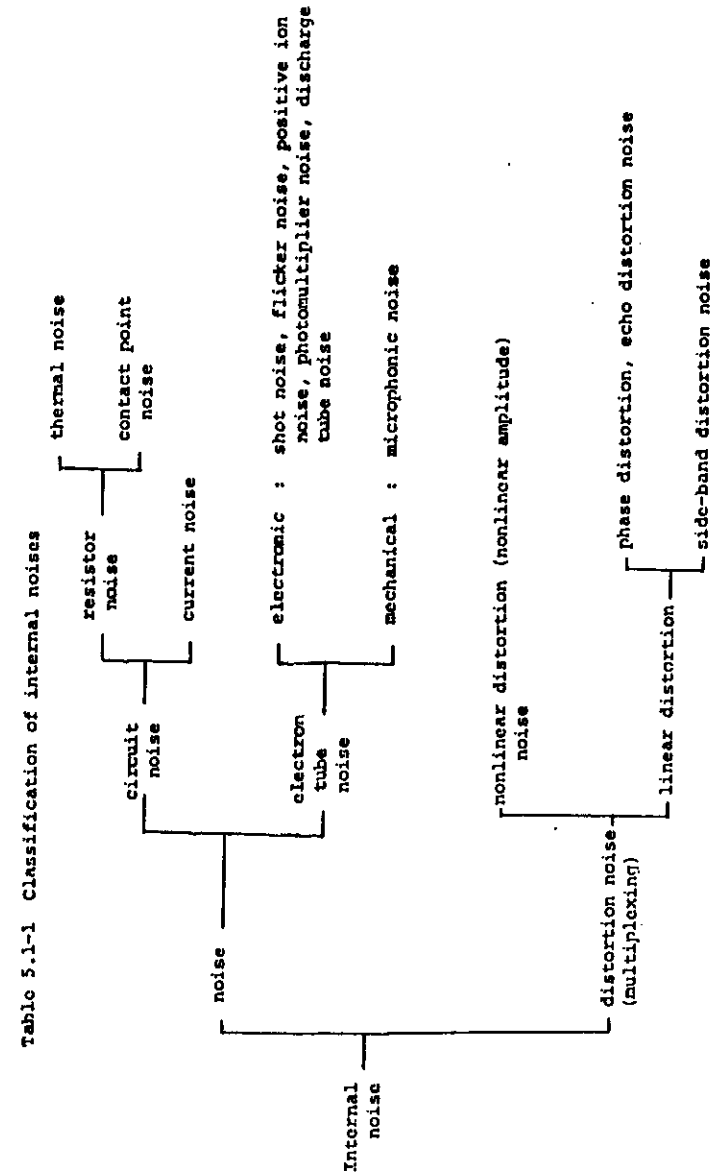
As the noises from vacuum tubes, transistors and diodes, there are shot noise, flicker noise and others, and the most important one among them is the shot noise. When the diode is operated in the temperature-limited state, the rms value of the fluctuating component of the plate current is given by

$$i_n^2 = 2 e I B \quad (5.1-3)$$

where e is the electronic charge, $I[\text{A}]$ is the average value (direct current component). This principle makes it possible for us to use this noise diode for the measurement of noise figure. As shown in Fig.5.1-1, this shot noise exhibits a flat frequency dependence in a range from 104 to 108 Hz. However, we have the flicker effect at lower frequencies, and the transit time effect becomes important at higher frequencies.

(c) Other noises

As indicated in Table 5.1-1, there are quasi cross-talk noises due to the nonlinear distortion in the multiplexing system.



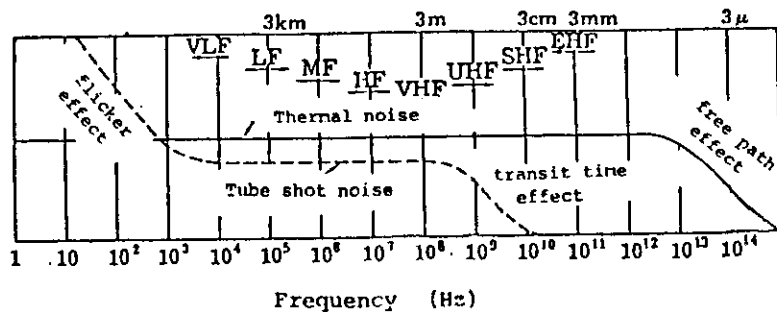


Fig.5.1-1 Frequency characteristic of internal noise.

5.2. Sensitivity of the receiver and the expression of internal noise figure

It is necessary for us to obtain the sufficient S/N at the receiver output for maintaining a good transmission quality in the communication. Even if there is no external noise, the signal level at the receiver input is influenced by the internal noise, and so the determination of R in Eq.(4.1-1) is closely associated with the receiver internal noise. When we make the overall consideration, we estimate the response of the receiver to both signal and noise, making it possible to choose which kind of modulation/demodulation scheme we should adopt. In an AM receiver, it is sufficient to consider only the S/N of the rms output. However, with the advent of an FM, PCM etc, the S/N ratio is not a complete measure of the noise properties of a signal, and so we have to use "noise figure" as well.

When we consider the S/N, we have to define the equivalent noise bandwidth of an amplifier and then to estimate the relationship between the noise figure and the overall sensitivity of the receiver.

5.3. Equivalent noise bandwidth of an amplifier

A widely used measure for the noises of radio receiver is the equivalent noise bandwidth. The noise of the receiver with an overall impedance Z and with a power gain G in a small bandwidth ΔB is given by

$$\Delta E_n^2 = Z^2 G \Delta I_n^2 = 2 e I Z^2 \Delta B G \quad (5.3-1)$$

The total integrated power over a bandwidth B_{eq} is

$$E_n^2 = 2 e I G \int_0^{B_{eq}} Z^2 df = 2 e I G Z_{max}^2 B_{eq} \quad (5.3-2)$$

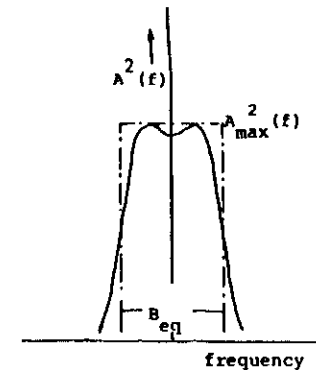


Fig.5.3-1 Equivalent noise bandwidth

Then, we have

$$B_{eq} = \int_0^{\infty} (Z^2 / Z_{max}^2) df = \int_0^{\infty} \{A(f)^2 / A_{max}(f)^2\} df \quad (5.3-3)$$

where A_{max} is the maximum amplification with the maximum gain, and A is the amplification at a frequency f. This equivalent bandwidth, B_{eq} is defined as having the same noise power as is actually developed by the amplifier output, as shown in Fig.5.3-1.

5.4. Noise figure

We define the ratio of available signal power to the available noise power at the input terminal of the amplifier as S_0/N_0 and the corresponding ratio at the output of the amplifier is referred to as S/N. As shown in Fig.5.4-1, the impedance at the input terminal (R_0) is assumed to be matched with the output load impedance (R). The noise figure F of a network is defined as

$$F = (S_0/N_0) / (S/N) \quad (5.4-1)$$

The available noise power N_0 from the input terminal is given by $N_0 = kTB$. G is the power gain of the circuit and so $G = S/S_0$. Then, Eq.(5.4-1) is rewritten as

$$F = \frac{N}{G k T B} \quad (5.4-2)$$

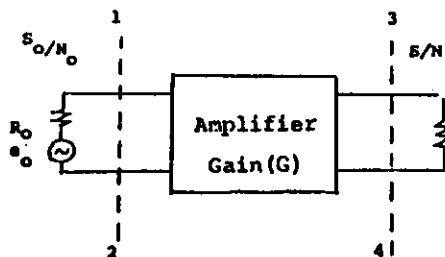


Fig.5.4-1 Explanation of noise figure of an amplifier.

The noise figure of a network is thus the ratio of the actual available output noise power to the available output noise power of an ideal network having the same gain characteristic. Therefore, the noise figure of an ideal network that generates no noise itself is $F=1$ and correspondingly the part of the noise figure of any network due to internally generated noise is $F-1$. Eq.(5.4-2) is rewritten as follows.

$$N = G k T B + G (F - 1) k T B \quad (5.4-3)$$

The first term on the right-hand side in Eq.(5.4-3) represents the noise coming from the input, and the second term stands for the noise generated within the amplifier. The signal to noise ratio when looking from the input is given by

$$\frac{S_o}{F k T B} = (\text{input signal power}) / (\text{total noise power transformed to the input terminal})$$

On the occasion when there exists an external noise, the S/N ratio at the output terminal is given as follows, by indicating the signal power through the antenna as S_o and the external noise as S_n ,

$$S/N = \frac{S_o}{S_n + (F-1) k T B} = \frac{S_o}{(\overline{EN} + F - 1) k T B} \quad (5.4-4)$$

Let us suppose that we have a few networks in cascade as shown in Fig.5.4-2, and we wish to know the noise figure of the combination in terms of the noise figures of the individual networks. The overall noise figure F is given as follows.

$$F = F_1 + \frac{F_2 - 1}{G_1} + \frac{F_3 - 1}{G_1 G_2} + \dots \quad (5.4-5)$$

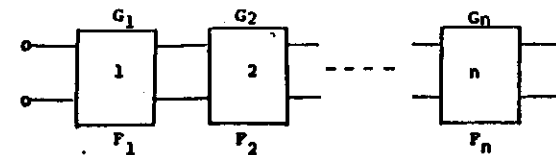


Fig.5.4-2 The noise figure of cascaded amplifiers.

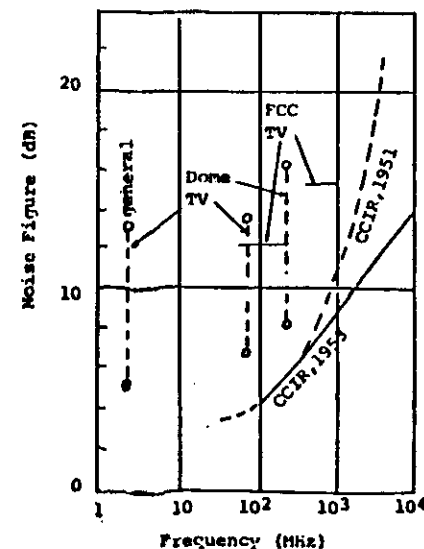


Fig.5.4-3 The noise figures of standard receivers.

where F_i ($i=1,2,3,\dots$) is the noise figure of the i th amplifier, and G_i , the corresponding gain. Hence, the overall F is primarily determined by F_1 at the first stage, and it is important to lower the noise figure of the first stage of amplifiers in cascade as possible as we can.

Examples of the noise figure F of radio receivers are illustrated in Fig.5.4-3.

5.5. Signal to noise ratio and its improvement

When the S/N ratio is smaller than the prescribed value, we cannot have satisfactory communications unless we take the following procedures.

(a) Raising the receiving power:

Two possible ways are considered; (1) an increase of the transmission power (though not so economical) and (2) an increase in the gain of the receiving antenna (it is required that EN' is small) and the lift-up of the antenna height at VHF and UHF.

(b) Lowering the noise figure of the receiver:

We adopt the low-noise figure receivers such as maser, parametric amplifiers, tunnel diodes, high-sensitivity receiving system.

(c) Improvement of selectivity of the receiver:

In order to suppress the noise power, we do not have the receiver bandwidth being more than necessary.

(d) Setting up the receiver site at a place with small external noise figure:

We try to suppress the man-made noise at the generation side.

(e) Adoption of the modulation/demodulation scheme which improves the S/N (wideband gain):

(f) We take the procedure so as to be free from the man-made noise from the receiving antenna, feeders, receivers, etc. Also, the insertion of noise suppressor.

By means of a combination of the procedures listed above, we have to consider the way how to achieve the most economical telecommunication in order to transmit the information or message. Then, the remaining problem will be how much we can improve the S/N ratio in each modulation scheme.

6. Description of random noises and their measurements

6.1. Measurement parameters

Because both natural and man-made noise are a random process, the characteristics of the noise can be described only in statistical terms and cannot be described by a deterministic waveform. Additionally, some noises are basically non-stationary, and so great care must be done in the planning and making of the measurements and in the interpretations of the results. We must measure long enough to obtain a good estimate of the required parameter, but be certain that the noise remains "stationary enough" during this period. We assume that the random process is stationary enough over some required time interval for us to obtain the statistics. Of course, how these statistics then change with time, day as well as with location, now becomes important.

The basic description of any random process is its probability density function (pdf). The first order pdf of the received interference process is almost always required to determine system performance. Although a random process, $x(t)$ is completely described if its hierarchy of distributions is known, there are other important statistical properties (important to communication systems) which are not immediately implied by this hierarchy. They include moments and distributions of level crossings of $x(t)$ within a time interval, moments and distributions of the time interval between successive crossings, distribution of extremes in the interval, and so on.

We now want to define, in a unified way, the noise parameters that have been measured and their interrelationships. For analysis of a communication system, the noise process of interest is the one seen by that part of our receiving system in which we attempt to extract information from the desired signal. The noise process $x(t)$ at the output of a narrow-band filter is given by

$$x(t) = v(t) \cos [\omega_c t + \phi(t)]$$

where $v(t)$ is the envelope process and $\phi(t)$ is the phase process as shown in Fig. 6.1-1. For atmospheric and man-made noise in the absence of discrete signals, ϕ is uniformly distributed; that is

$$p(\phi) = \frac{1}{2\pi}, \quad -\pi \leq \phi \leq \pi$$

Therefore, we will concentrate on the statistics of the envelope process, $v(t)$. In general, for system analysis, the required statistics that determine performance are either the envelope statistics directly or are obtainable from the envelope and phase statistics. For noise from some discrete sources, or for general background noise plus interfering signals, $\phi(t)$ is not uniformly distributed, and the statistics of the $\phi(t)$ process must also be known.

Let $x(t)$ be a white Gaussian process as an example (see Fig. 6.1-1), then

$$p(x) = \frac{1}{\sqrt{\pi x_0}} \exp \left[-\frac{x^2}{x_0} \right]$$

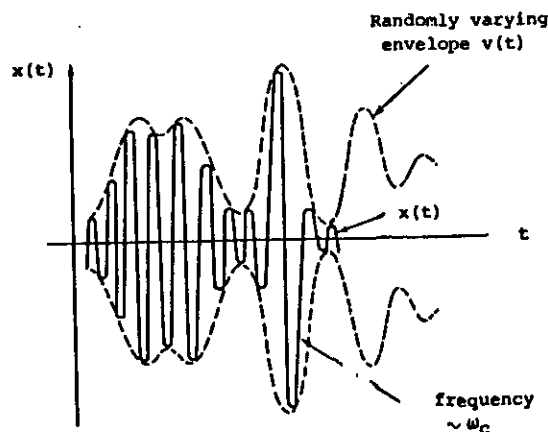


Fig.6.1-1 Noise waveform at the output of a narrowband filter

$$p(v) = \frac{2v}{x_0} \exp \left[-\frac{v^2}{x_0} \right], \quad v \geq 0$$

$$p(\phi) = \frac{1}{2\pi}, \quad -\pi \leq \phi \leq \pi$$

where x_0 is the noise power spectral density [W/Hz]. That is, the envelope voltage v is Rayleigh distributed and the phase is uniformly distributed.

Fig.6.1-2 shows the noise envelope of a sample of radio noise along with definitions of the various noise parameters that have been measured. From Fig.6.1-2, we have

The amplitude probability distribution (APD) is the fraction of the total measurement time, T for which the envelope was above level v_i :

$$D(v_i) = \text{Prob} [v \geq v_i] = 1 - P(v_i)$$

where $P(v)$ is the cumulative distribution function. The pdf of v is given by the derivative of $P(v)$.

The average crossing rate characteristic (ACR) is the average number of positive crossings of level v_i = total number/ T . For impulsive noise and at high envelope voltage levels, an average noise pulse rate (pulses/sec) at the receiver input can be inferred from the ACR. The requirement for the pulse rate to be essentially equal to the ACR is that the noise envelope (at the level v_i) be composed of isolated filter impulse responses.

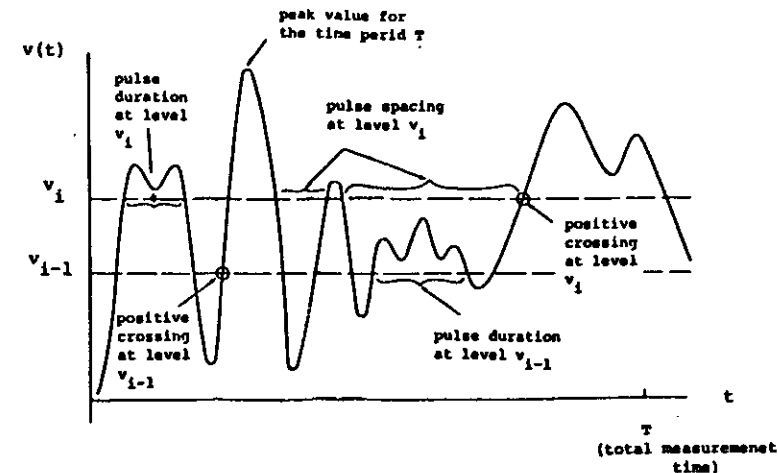


Fig.6.1-2 Noise envelope of a sample of radio noise

The noise amplitude distribution (NAD) is a term that has been used to describe a method of presenting ACR data as a function of threshold level, where it is assumed that a positive level crossing corresponds to the occurrence of a pulse at the receiver input. Note that the NAD is not the distribution of a random variable, but rather the NAD is a method of presenting impulsive noise ACR data, where the inference is made that each positive level crossing represents an impulse at the receiver input which exceeds that particular level.

The pulse spacing distribution (PSD) for level v_i is the fraction of pulse spacings at level v_i that exceeds time τ . That is, the PSD is the distribution for the random variable τ .

The pulse duration distribution (PDD) for level v_i is the fraction of pulse durations at level v_i that exceeds time τ .

To specify time dependence in the received waveform, the autocorrelation function, $R(\tau)$ is used.

$$\begin{aligned} R(\tau) &= \int_{-\infty}^{\infty} \int_{-\infty}^{\infty} v_1 v_2 p_2(v_1, v_2, \tau) dv_1 dv_2 \\ &= \lim_{T \rightarrow \infty} \frac{1}{T} \int_0^T v(t) v(t+\tau) dt \end{aligned}$$

where v_1 is the $v(t)$ at time t_1 , and v_2 is $v(t)$ at t_2 , and $\tau = t_2 - t_1$, with $p_2(v_1, v_2)$ the 2nd order pdf of $v(t)$. The autocovariance of $v(t)$ is the covariance of the random variables $v(t_1)$ and $v(t_2)$. For zero mean processes, the autocorrelation and autocovariance are identical.

The power spectral density, $S(\omega)$, for a stationary random process is given by the Fourier transform of $R(\tau)$. This is similar to the Fourier transform pair relationship between the time domain representation and the

frequency domain representation of deterministic waveforms. Note, however, that while for deterministic waveforms the spectrum gives the amplitude of each frequency component and its phase, no phase information is possible for the spectrum of a random process. If the process is yime independent (correlated only for $\tau=0$), then

$$R(\tau) = X_0 \delta(\tau - 0)$$

and $S(\omega) = X_0$ (white noise).

The average envelope voltage is termed the expected value of v , $E[v]$;

$$v_{av} = E[v] = \frac{1}{T} \int_0^T v(t) dt = - \int_0^\infty v dD(v)$$

where

$$-dD(v) = p(v)dv$$

The rms voltage squared, (proportional to energy, or power) $E[v^2]$, is

$$v_{rms}^2 = E[v^2] = \frac{1}{T} \int_0^T v^2(t) dt = - \int_0^\infty v^2 dD(v)$$

The average logarithm of the envelope voltage, $E[\log v]$, is

$$v_{log} = E[\log v] = \frac{1}{T} \int_0^T \log v(t) dt = - \int_0^\infty \log v dD(v)$$

The peak voltage for time period T is the maximum of $v(t)$ during T .

Quasi-peak voltage: The noise envelope is passed through a circuit with a very short charging time and long discharging time as shown in Fig. 6.1-3. The quasi-peak voltage, v_{qp} , is the average voltage over time T of the quasi-peak circuit output waveform. Since the quasi-peak voltage depends on both the amplitude and time behaviour of the interfering noise, it has found use in subjectively determining system performance for systems whose signals have redundancy, especially voice systems.

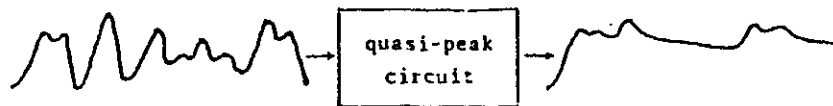


Fig. 6.1-3 The quasi-peak detector circuit.

Because the rms voltage level can be given in absolute terms (i.e. rms available field strength or available power), it is common to refer the other envelope voltage levels to it. The dB difference between the average voltage and the rms voltage is termed V_d ,

$$V_d = -20 \log \frac{v_{av}}{v_{rms}}$$

The dB difference between the antilog of the average log of the envelope voltage and the rms voltage is termed L_d ,

$$L_d = -20 \log \frac{10^{v_{log}}}{v_{rms}}$$

The dB difference between the v_{qp} and v_{rms} is termed Q_d ,

$$Q_d = 20 \log \frac{v_{qp}}{v_{rms}}$$

Knowledge of the behaviour of the above statistics with time (hour to hour, say) and location is also important.

Figs. 6.1-4 and 6.1-5 show a 200 ms sample of atmospheric noise envelope, taken from a 6 min noise recording at 2.5 MHz in a 4 kHz bandwidth, and the autocovariance for this sample. Figs. 6.1-6, 6.1-7, 6.1-8 and 6.1-9 show the APD, ACR, PSD, and PDD for this 6-minute sample of noise. In Fig. 6.1-6 the dashed curve (Rayleigh distribution) is the distribution of the receiving noise at 2.5 MHz.

In addition to those above, there are the following relationships between the various noise statistics. In general, the ACR at the level v_i , $c(v_i)$ is given by,

$$c(v_i) = \frac{1}{2} \int_{-\infty}^{\infty} |\dot{v}| p(v_i, \dot{v}) d\dot{v}$$

where the $\dot{v}(t)$ process is the derivative (with respect to t) of the $v(t)$ process (note that "derivative" of a random process must be defined in a generalized probabilistic way) and $p(v, \dot{v})$ is the joint probability density of v and \dot{v} .

In the special case where, at the level v_i , the envelope is composed of isolated filter impulse responses, $c(v_i)$ can be given by

$$c(v_i) = \alpha_{eq} p(v_i)$$

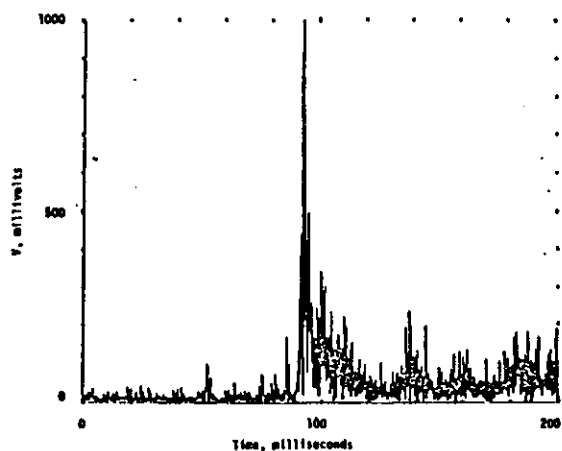


Fig.6.1-4 Randomly selected 200ms sample of atmospheric noise envelope from a 6-min noise recording at 2.5MHz in a 4kHz bandwidth.

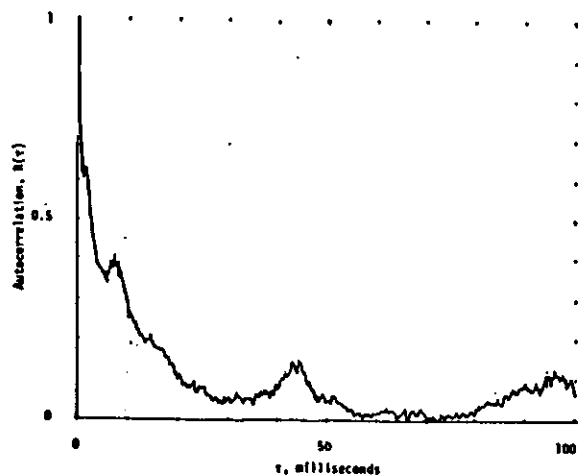


Fig.6.1-5 Autocorrelation for the noise sample of Fig.6.1-4.

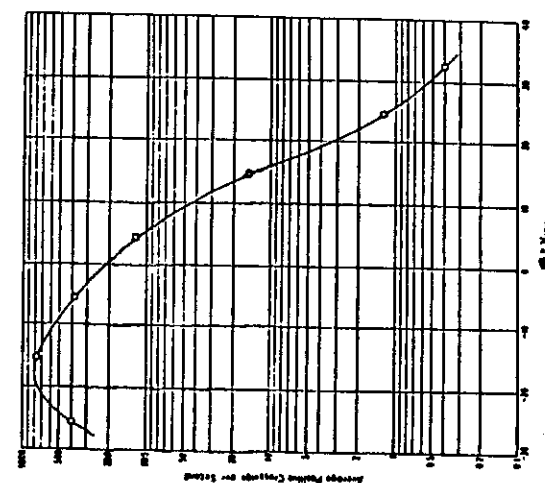


Fig.6.1-7 Average positive crossing rate (ACR) for the sample of noise of Fig.6.1-6.

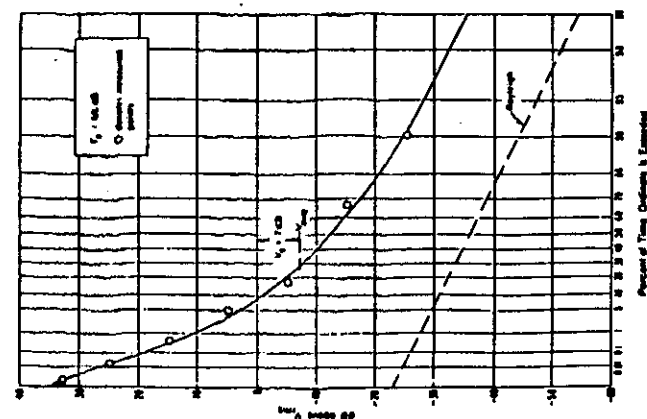


Fig.6.1-6 Amplitude probability distribution for a 6-min sample of atmospheric noise recorded at 2.5MHz in a 4 kHz bandwidth.

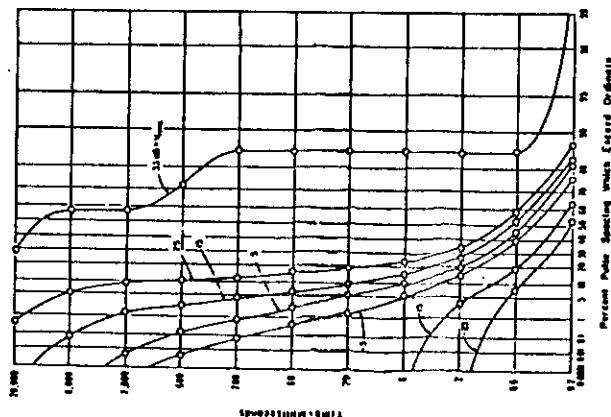


Fig. 6.1-9 Pulse spacing distributions (PSD) for the sample of noise of Fig. 6.1-6.

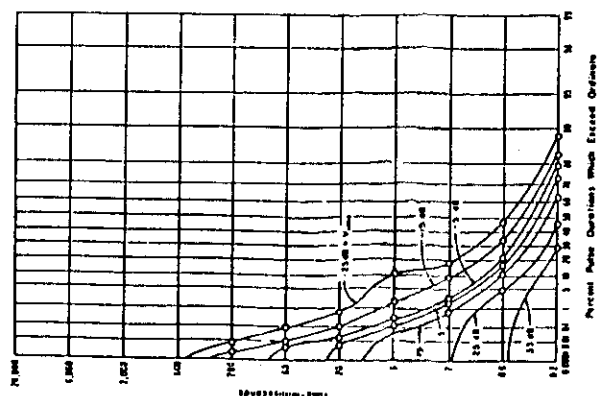


Fig. 6.1-8 Pulse duration distributions (PDD) for the sample of noise of Fig. 6.1-6.

where $p(v_i)$ is the probability density of v at the level v_i , α is a non-dimensional constant on the order of unity that depends on the shape of the receiver bandpass characteristic (or equivalently, the receiver impulse response) and the power spectrum of the noise within the band, and B_{eq} is the effective noise power bandwidth.

The fraction of time the noise envelope is above v_i is given by

$$D(v_i) \approx c(v_i) E(\tau_i)$$

where $E(\tau_i)$ is the mean value for the pulse width distribution at v_i .

6.2. Measurement techniques

The noise measurement techniques incorporate four basic elements; an antenna, receiver, detector and measuring device. The antenna is a "standard" one or the antenna of an operational system. The receiver is a type consistent with the existing state-of the art tuned radio for heterodyne or a superheterodyne. An electro-mechanical or vacuum tube voltmeter has been used as the measuring device. The detector chosen has been the one that gives the desired statistical parameter- peak voltage, quasi-peak voltage, square law (voltage squared or calorimeter) or average voltage. The performance and especially differences in performance of these diverse detectors, are understood. For single-frequency, continuous wave inputs, the four detectors, suitably calibrated, give comparable readings. In all other general cases, it is difficult to correlate readings from the several diverse detectors unless there is a priori independent knowledge of the waveform of the received noise. The factors determining the transient response of the measurement equipment are (1) the bandwidth of IF receiver (B), (2) charge time constant of the detector (T_c), (3) discharge time constant of the detector, T_d and (4) the mechanical time constant of the measuring device, T_m , as shown in Fig. 6.2-1. The measuring device of radio noise is classified as follows from the standpoints of the characteristics of detectors.

(1) Envelope detector:

The fundamental behavior of this detector is strongly dependent on B , T_c and T_d . When an impulse is incident on the measuring equipment, the output of the IF amplifier exhibits a pulse waveform with its duration of about $1/B$ as in Fig. 6.2-2. When this pulse wave is fed to the detector, the output waveform exhibits an envelope of the IF amplifier output as shown in Fig. 6.2-2(a) when both T_c and T_d are sufficiently small compared with $1/B$ (but larger than the reciprocal of the IF frequency). This detector is called an "envelope detector", and this kind of detector is used as normal receivers, electric field intensity measuring instrumentations, spectrum analyzers, and so on.

(2) Peak value detector:

When T_d is sufficiently large, the detector shows a discharge only very slightly and then the detector gives rise the output of a peak value (maximum) of the IF output signal as shown in Fig. 6.2-2(b). This is the "peak detector". It was difficult to build a detector with extremely large T_d in the old days. However, the measurement of radio noises by means of the peak detector is considered as being important in recent days with the advent of the digital communications.

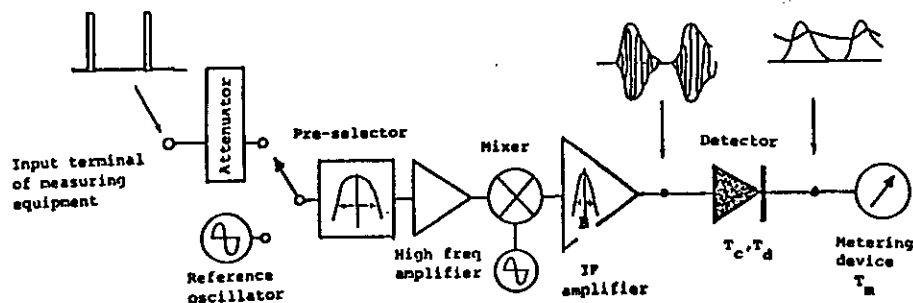


Fig.6.2-1 Fundamental construction of radio noise measuring equipment.

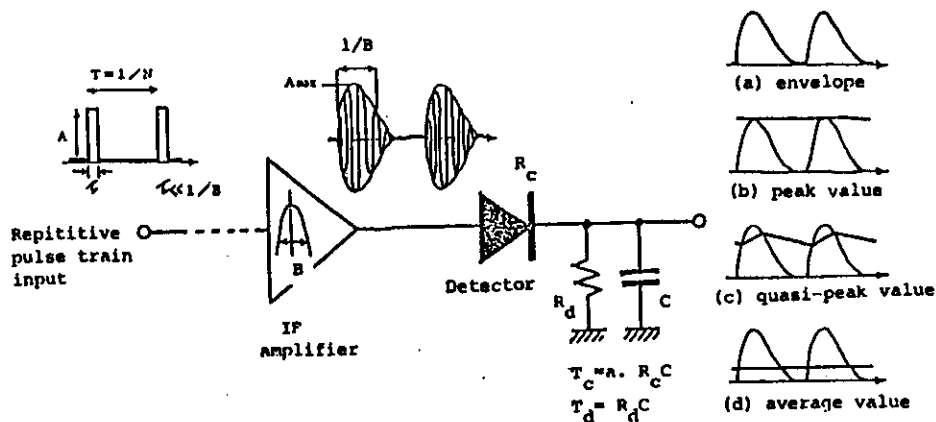


Fig.6.2-2 Response outputs of different kinds of detectors for pulse train input.

(3) Quasi-peak value detector:

When both T_C and T_d are larger than $1/B$, the detector cannot follow exactly the envelope of IF output, and we have the detector output as in Fig.6.2-2(c) with having the charging and discharging characteristics of the detector. This is called a "quasi-peak value detector", which is in current use nowadays. The response of this quasi-peak value detector for radio noises is strongly dependent on the bandwidth of the IF amplifier (B) and the charging and discharging time constants of the detector (T_C, T_d) (this point being quite different from the peak and average value detectors), and so the fundamental characteristics are strictly regulated by CISPR at the different frequency ranges (see Table 6.2-1).

The responses of this quasi-peak value detector to different kinds of input waves (sine wave, Gaussian noise and pulse trains) are summarized in Table 6.2-2. The detection efficiency (P_s) for a sine wave is approximately unity as seen in Table 6.2-2. The corresponding detection efficiency (P_r) for Gaussian random noise is also given in the table.

The most important factor specifying the quasi-peak value detector is its response to pulse trains, because this pulse response is strongly influenced by the fundamental characteristics (B, T_C, T_d etc), the nonlinear effect of the amplifier, etc. The pulse train is characterized by the repetition (repetition frequency, N) of equal amplitude pulses (amplitude, A ; width, τ), and the detection efficiency, P_p for pulse train is numerically calculated in Fig.6.2-3 as a function of α (inversely proportional to N). By measuring the pulse train noises ($N=100$ Hz, $A\tau=0.044$ $\mu\text{V}\cdot\text{sec}$) by means of the measuring equipments in the bands C and D in Table 6.2-1, Table 6.2-2 gives $P_s=0.99$ and $P_p=0.27$ is obtained from Fig.6.2-3. Then, the metering value of the quasi-peak value detector becomes ~ 2 mV. So, the CISPR regulation requires that the response of the radio noise measuring instrumentation with quasi-peak detector should be within $\pm 1.5\text{dB}$ around the response for the sine wave with rms value of 2 mV.

(4) Average value detector:

The fundamental construction of the average detector is that we obtain the average of the output signal of the IF amplifier (see Fig.6.2-2(d)) by passing through the narrow-band low-pass filter after the envelope detection. Some average value detectors are composed of the half-wave rectification of the IF output, followed by the narrow-band low-pass filter. Since this average value detector is suitable for the level measurement for signals with small amplitude variations such as broadcasting and communication signals, it is equipped in the electric field intensity measuring equipment. The measurement of radio noises by means of the average value detectors has seldom been made, but recently the CISPR

Table 6.2-1 Fundamental characteristics of radio noise measuring instrumentation (CISPR Pub. 16)

Frequency Band	A	B	C	D
Frequency range	10-150kHz	0.15-30MHz	30-300MHz	300-1000MHz
Bandwidth (B)	200 Hz	9 kHz	120kHz	120 kHz
Charging time constant (T_C)	45 ms	1 ms	1 ms	1 ms
Discharging time constant (T_d)	500 ms	160 ms	550 ms	550 ms
Mechanical time constant (T_m)	160 ms	160 ms	100 ms	100 ms

Table 6.2-2 Detection efficiency of quasi-peak field measuring instrumentation for sine waves and Gaussian noises.

Frequency Band	A	B	C	D
Freq. rang	10-150kHz	0.15-30MHz	30-300MHz	300-1000MHz
a	2.98	3.94	4.07	4.07
P_g	0.813	0.970	0.987	0.987
P_r	0.955	1.63	1.88	1.88

$a = T_C / (R_C C)$, P_g : detector efficiency for sine waves,
 P_r : detector efficiency for Gaussian noise.

and FCC have recently suggested simultaneous use of the measurement by this average value detector in addition to the quasi-peak value measurement because of the advent of the use of digital equipments.

The response of radio noise measuring instrumentation with average detector is specified as follows in the lights of the CISPR specification. The value indicated by the average value measuring system should be $\sim 2\text{mV}$ for the pulse train with repetition frequency $N[\text{Hz}]$ and with amplitude $A_r = (1.4/N) \text{ mV}\cdot\text{sec}$. And, the pulse amplitude A for the pulse train input so as to keep the meter value constant, is regulated to be inversely proportional to N . The amplitude of the pulse train input is plotted in Fig.6.2-4 for radio noise measuring system with the quasi-peak value and average value detectors. The response of the average value detector to a sine wave and pulse train is independent of the bandwidth, B of the measuring system, and so there is no specific regulation on the bandwidth.

(5) Rms detector:

The root-mean-square method of detection has a growing utility in problems of current interest and has low implementation cost, large dynamic range, and wide frequency-band response. Of course, rms detection is required to measure the basic noise parameter, mean power. Commercial rms detectors are available with sufficient dynamic range for the measurement of impulsive noise. Several commercial products have been marketed that use rms detectors to measure the power in pulses as short as 100 ns and frequencies as high as 18 GHz. There are unsolved problems in measuring impulsive interference when it is extremely infrequent, of extremely short duration, or swept in frequency. Recourse to transient instruments (i.e., broadband oscillographs, storage or sampling oscilloscopes, tape loop recorders, etc) with wide dynamic response system capability is necessary to investigate the man-made transient interference often encountered in present-day systems. The problem of measuring signals of low duty cycle and single transients with duration below 1 μs is introduced.

For analysis and/or design of communication systems, greater knowledge of the received noise process is greatly required than that given by the above detector outputs (average, rms, etc). Techniques for measurements of these more detailed statistics (e.g., probability density functions, autocorrelation, etc) vary greatly and range from the analog record-and-A/D conversion-large scale computer analysis technique to those using specialized electronic circuitry. Techniques for making detailed statistical measurements are discussed and summarized by Bendat and Piersol (1971). Until recently, the capability to make such detailed statistical measurements has resided in a few Government and private research laboratories using specially developed equipment. Commercial equipment is now available for detailed statistical measurements of impulsive noise.

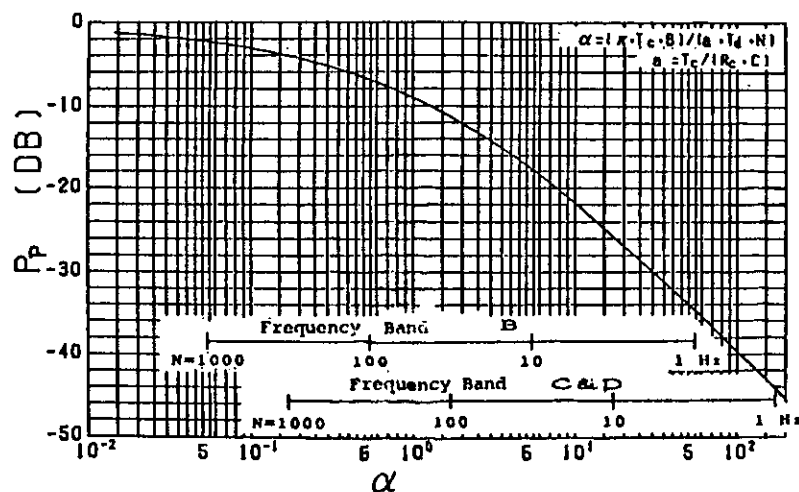


Fig. 6.2-3 Detection efficiency of quasi peak-field measuring instrumentation for pulse trains.

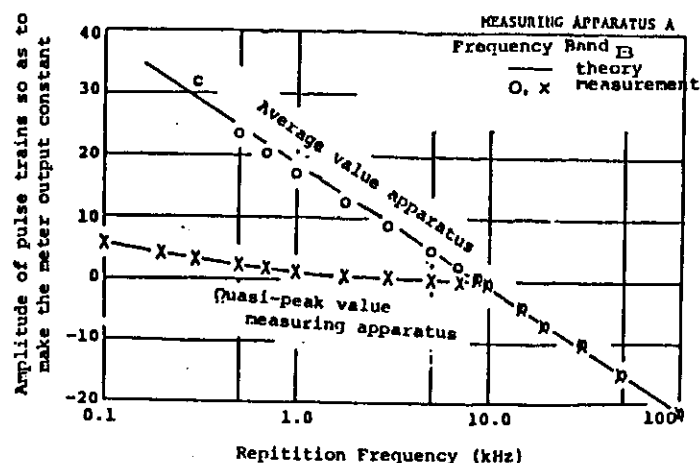


Fig. 6.2-4 The response to pulse trains of the radio interference apparatus.

References

- Bendat, J.S., and A.G. Piersol, Random Data; Analysis and Measurement Procedures, Wiley-Interscience, New York, 1971.
- CCIR, World distribution and characteristics of atmospheric radio noise, CCIR Report 322, Intl Telecommunication Union, Geneva, 1964.
- CCIR, Operating noise threshold of a radio receiving system, CCIR Report 413, ITU, Geneva, 1967.
- CCIR, Definitions of interference, CCIR Report 529, ITU, Geneva, 1974.
- CISPR, Specifications for CISPR radio interference measuring apparatus for the frequency range 0.15 MHz to 30 MHz, Second edition, CISPR Publication 31, 1972.
- CISPR, Specifications for CISPR radio interference measuring apparatus for the frequency range 25 MHz to 300 MHz, Second edition, CISPR Publication 2, 1975.
- Hagn, G.H., Man-made noise, in Handbook of Atmospheric, Vol. I, ed. by H. Volland, CRC Press, Boca-Raton, p.329-355, 1982.
- Kimpara, A., Atmospheric, Kawade Shobo, 1944 (in Japanese).
- Kraus, J.D., Radio Astronomy, McGraw-Hill Book Comp., New York, 1966.
- Lewis, E.A., High frequency radio noise, in Handbook of Atmospheric, ed. by H. Volland, CRC Press, Boca-Raton, p.252-288, 1982.
- Middleton, D., Statistical-physical models of urban radio noise environments, Part I: Foundations, IEEE Trans. EMC, EMC-14, 36-56, 1972.
- Seki, H., Noises, Iwanami Pub. Comp., 1954 (in Japanese).
- Skomal, E.N., Man-made Radio Noise, Van Nostrand Reinhold Comp., New York, 1978.
- Spaulding, A.D., and R.T. Disney, Man-made radio noise, Part I: Estimates for business, residential, and rural areas, U.S. Dept of Commerce, O.T. Report 74-38, O.T., 1974.
- Spaulding, A.D., Atmospheric noise and its effects on telecommunication system performance, in "Handbook of Atmospheric", Vol. I, ed. by H. Volland, CRC Press, Boca-Raton, p.289-328, 1982.
- Suglura, A., and Y. Yamanaka, Measurements of Electromagnetic interferences, unpublished manuscript.
- URSI, The measurement of characteristics of terrestrial radio noise, URSI Special Report No. 7, Elsevier Pub. Comp., Amsterdam, 1962.